

# Behavior of Sulfur Abundances in Metal-Poor Giants and Dwarfs

Masahide Takada-Hidai

Liberal Arts Education Center, Tokai University, 1117 Kitakaname, Hiratsuka, Kanagawa,  
Japan 259-1292

[hidai@apus.rh.u-tokai.ac.jp](mailto:hidai@apus.rh.u-tokai.ac.jp)

Yoichi Takeda

Institute of Astronomy, The University of Tokyo, Mitaka, Tokyo, Japan 181-0015

[takedayi@cc.nao.ac.jp](mailto:takedayi@cc.nao.ac.jp)

Shizuka Sato

Department of Aeronautics, School of Engineering, Tokai University, 1117 Kitakaname,  
Hiratsuka, Kanagawa, Japan 259-1292

[shizuka@apus.rh.u-tokai.ac.jp](mailto:shizuka@apus.rh.u-tokai.ac.jp)

Satoshi Honda

National Astronomical Observatory, Mitaka, Tokyo, Japan 181-8588

[honda@optik.mtk.nao.ac.jp](mailto:honda@optik.mtk.nao.ac.jp)

Kozo Sadakane

Astronomical Institute, Osaka Kyoiku University, Kashiwara, Osaka, Japan 582-8582

[sadakane@cc.osaka-kyoiku.ac.jp](mailto:sadakane@cc.osaka-kyoiku.ac.jp)

Satoshi Kawanomoto

Department of Astronomy, School of Science, The University of Tokyo, Bunkyo-ku, Tokyo,  
Japan 113-0033

– 2 –

`kawanomo@optik.mtk.nao.ac.jp`

Wallace L. W. Sargent and Limin Lu

Department of Astronomy, California Institute of Technology, Mail Stop 105-24, Pasadena,  
CA 91125

`wws@astro.caltech.edu`

and

Thomas A. Barlow

Infrared Processing and Analysis Center, California Institute of Technology, Mail Stop  
100-22, Pasadena, CA 91125

`tab@ipac.caltech.edu`

Received \_\_\_\_\_; accepted \_\_\_\_\_

Submitted to *Astrophys. J.*

## ABSTRACT

LTE and NLTE abundances of sulfur in 6 metal-poor giants and 61 dwarfs (62 dwarfs, including the Sun) were explored in the range of  $-3 \lesssim [\text{Fe}/\text{H}] \lesssim +0.5$  using high-resolution, high signal-to-noise ratio spectra of the S I 8693.9 Å and 8694.6 Å lines observed by us and measured by François (1987, 1988) and Clegg et al. (1981). NLTE effects in S abundances are found to be small and practically negligible. The behavior of [S/Fe] vs. [Fe/H] exhibits a linear increasing trend without plateau with decreasing [Fe/H]. Combining our results with those available in the literature, we find that the slope of the increasing trend is  $-0.25$  in the NLTE behavior of [S/Fe], which is comparable to that observed in [O/Fe]. The observed behavior of S may require chemical evolution models of the Galaxy, in which scenarios of hypernovae nucleosynthesis and/or time-delayed deposition into interstellar medium are incorporated.

*Subject headings:* Galaxy: evolution — nucleosynthesis, abundances — stars: abundances — stars: atmospheres — stars: Population II

## 1. Introduction

The behavior of  $\alpha$ -elements such as oxygen, magnesium, silicon, sulfur, calcium, and titanium in metal-poor halo and disk stars provides us with very useful information and constraints for exploring stellar nucleosynthesis and chemical evolution of the Galaxy in the early phase, since these elements are believed to be produced mainly by type II supernovae (SNe II) of massive stars (e.g. Timmes, Woosley, & Weaver 1995; Chiappini et al. 1999; Carretta, Gratton, & Sneden 2000) and are fossilized in stars which have been born at various epochs of the Galaxy evolution.

Numerous abundance works have been carried out for these elements (e.g. see a review of McWilliam 1997). It is well known that the  $\alpha$ -elements, except for O and S, show a general trend of abundances such that  $[\alpha\text{-element}/\text{Fe}]$  increases with decreasing metallicity  $[\text{Fe}/\text{H}]$  down to about  $-1$  dex, and forms a plateau with  $[\alpha\text{-element}/\text{Fe}] \sim 0.3 - 0.5$  dex in the range of  $[\text{Fe}/\text{H}] < -1$  dex. Here we define  $[\text{A}/\text{B}] \equiv \log (\text{A}/\text{B})_{\text{star}} - \log (\text{A}/\text{B})_{\text{sun}}$  for the elements of A and B and use it throughout the text hereafter. The behavior of  $[\text{O}/\text{Fe}]$  against  $[\text{Fe}/\text{H}]$  is controversial, i.e. whether  $[\text{O}/\text{Fe}]$  shows a plateau (e.g. Barbuy 1988; Fulbright & Kraft 1999) or a steady linear increase with decreasing  $[\text{Fe}/\text{H}]$  (e.g. Boesgaard et al. 1999; Israeli et al. 2001; Takeda et al. 2002).

As for the behavior of S among metal-poor stars, it is not well understood because there are only four previous works dealing with a larger number of stars: Clegg, Lambert, & Tomkin (1981) and François (1987, 1988) for a total number of 44 dwarfs and one giant star; Prochaska et al. (2000) for nine thick disk dwarfs. These works analyzed S abundances in the metallicity range,  $-1.6 \lesssim [\text{Fe}/\text{H}] \lesssim +0.5$ , but mostly in  $[\text{Fe}/\text{H}] > -1$ . The scarcity of the S abundance works is mainly due to the difficulty in observing the S lines available to abundance analysis. There are no strong lines in the visual region suitable enough for analysis, but there are a few relatively strong lines of S I (multiplet number 6) in the near-infrared region of  $8670 - 8700 \text{ \AA}$ . Among the S I (6) lines, the strongest line at  $8694.641 \text{ \AA}$  and a weak line at  $8693.958 \text{ \AA}$  are free from blending with lines of other ions such as Si I and Fe I, while the remaining lines are blended with such ions. Even the strongest line at  $8694.6 \text{ \AA}$  generally becomes very weak for stars with effective temperature ( $T_{\text{eff}}$ ) of  $T_{\text{eff}} < 5500 \text{ K}$  and with metallicity of  $[\text{Fe}/\text{H}] < -0.5$  (cf. François 1987, 1988).

Among these previous studies, François (1988) suggested that  $[\text{S}/\text{Fe}]$  becomes overabundant and constant in the halo stars with a value of  $+0.6$  dex in the metallicity range of  $-1.6 < [\text{Fe}/\text{H}] \lesssim -1$ , while Prochaska et al. (2000) found no indication of a

significant overabundance of  $[S/Fe]$  with a mean value of  $+0.11 \pm 0.08$  dex and no trend with metallicity in the range of  $-1.2 \lesssim [Fe/H] \lesssim -0.3$ . Prochaska et al. (2000) also postulated that a more careful, extensive stellar abundance analysis of S in metal-poor stars is warranted since S is one of important elements in quasar absorption-line studies.

Very recently, Israelian & Rebolo (2001) analyzed the S abundances in six metal-poor stars with metallicities in the range of  $-3 < [Fe/H] < -0.2$  using observational data of S I lines at 8694 Å. Their results indicate a monotonic increase of  $[S/Fe]$  as  $[Fe/H]$  decreases, reaching  $[S/Fe] \sim 0.7 - 0.8$  below  $[Fe/H] = -2$ .

Takeda et al. (2002; hereafter Paper I) also very recently reported the abundance analysis of S for very metal-poor giants with  $[Fe/H] \lesssim -1.5$  observed with the High Resolution Echelle Spectrometer (HIRES; Vogt 1994) of the 10 m Keck I telescope as a byproduct in the oxygen abundance study. It is suggested that  $[S/Fe]$  increases linearly with decreasing  $[Fe/H]$ , which is just the same trend as found in Israelian & Rebolo (2001), and this behavior resembles that of O. However, Paper I's results of S are yet preliminary and should be superseded with those of this study.

In this paper, in order to explore the behavior of S in the metallicity range of  $-3 \lesssim [Fe/H] \lesssim +0.5$ , we carried out extensive LTE abundance analyses of S for the six samples of very metal-poor stars in Paper I observed with the Keck I HIRES (hereafter, the HIRES sample) and of metal-poor dwarfs observed at the Okayama Astrophysical Observatory (hereafter, the OAO sample). We also re-analyze the data of dwarfs observed by Clegg et al. (1981) and François (1987, 1988) based on our system of analysis to eliminate the systematic differences between our and the previous analyses. We further perform the non-LTE (NLTE) abundance analysis for all these sample stars to examine how the NLTE abundances of S behave and how the NLTE affects the LTE abundance determination, since a NLTE analysis of S abundance in metal-poor stars has not been done until now.

## 2. Observations and Measurements

The basic data of the sample stars of HIRES, OAO, François (1987, 1988), and Clegg et al. (1981) are presented in Table 1. Spectral types in the third column were adopted from the SIMBAD database, operated at CDS, Strasbourg, France. Parallaxes  $\pi$  and apparent  $V$  magnitudes in the fourth and sixth columns, respectively, were taken from the *Hipparcos* Catalogue (Perryman et al. 1997).

The CCD spectroscopic observations of the HIRES sample were carried out in 1997 and 1999 using HIRES on the Keck I telescope for the wavelength range,  $6330 \text{ \AA} \lesssim \lambda \lesssim 8760 \text{ \AA}$ , with resolution  $R = 45000$  and  $60000$ , respectively. The journal of observations is presented in Table 1 of Paper I, and the data reduction was performed with the MAKEE package developed by one of us (T.A. Barlow) for HIRES data. The reader is asked to refer to Paper I for the details of observations and data reduction. The S/N ratios in the wavelength region around the S I lines at  $8694 \text{ \AA}$  are estimated to be  $190 - 410$  in the sample stars. The low values are mainly due to the difficulty of complete removal of fringes in the spectra. The observed spectra in the vicinity of the S I lines are shown in Figures 1a – 1f.

The OAO sample of 25 dwarfs and the Moon were observed in 1997 and 1998 using the Coude spectrograph of the 188 cm telescope at the Okayama Astrophysical Observatory (OAO), National Astronomical Observatory of Japan. The wavelength range observed is  $\lambda \lambda 8400 - 8830 \text{ \AA}$ , and the resolution  $R \sim 24500$  at  $8700 \text{ \AA}$ . The CCD data were reduced with the IRAF<sup>1</sup> package, following the standard procedure of extracting one-dimensional spectra. The S/N ratios around  $8700 \text{ \AA}$  are in the range of  $120 - 400$ , but mostly between  $200 - 350$ .

---

<sup>1</sup>IRAF is distributed by the National Optical Astronomy Observatories, which is operated by the Association of Universities for Research in Astronomy, Inc., under cooperative agreement with the National Science Foundation.

Equivalent widths ( $W_\lambda$ ) of the two blend-free S I lines at 8693.958 Å and 8694.641 Å in spectra of the HIRES sample were measured by Gaussian fitting (or by direct integration if necessary) using the *splot* task of IRAF, and are listed in the HIRES sample entry of Table 5. It turned out that our  $W_\lambda$  values of the S I 8694.641 Å excellently agree with those measured in Paper I for the sample stars, except for the giant star HD 88609. While the  $W_\lambda$  value for HD 88609 was estimated to be 1.9 mÅ as an uncertain value in Paper I, it should be replaced with our measurement ( $< 2.2$  mÅ) as an upper limit corresponding to the noise level with a S/N ratio of  $\sim 230$ , because the S I 8694.641 Å line is not detected at this noise level, as seen in Figure 1c. Since the spectral resolution  $R$  of data of the OAO sample is not high enough to separate two S I lines clearly, two blended S I lines were regarded as one line and its  $W_\lambda$  was measured by a direct integration using the *splot* task of IRAF. The results are given in the seventh column of Table 4. We also measured  $W_\lambda$  of six Fe I lines in the OAO sample by Gaussian fitting using the *splot* task of IRAF, and listed them in Table 3. Values of  $W_\lambda$  measured by François (1987, 1988) and Clegg et al. (1981) for two S I lines are summarized in Table 5, and also those by François (1987, 1988) for two or three Fe I lines in Table 3. The  $W_\lambda$  data for Fe I lines are not available in Clegg et al. (1981).

Our OAO sample overlaps with nine stars among the samples of François (1987, 1988) and Clegg et al. (1981), so that the sample of this study consists of six giants and 61 dwarfs (62 dwarfs, including the Sun) in total.

### 3. Abundance Analyses

Abundance analyses were carried out using Kurucz's (1993) ATLAS9 line-blanketed model atmospheres, based on which the atmospheric models of individual stars were constructed by interpolation in terms of atmospheric parameters of effective temperature  $T_{\text{eff}}$ , surface gravity  $\log g$ , and metallicity [Fe/H]. In this section we describe the

determinations of atmospheric parameters and the analyses of Fe and S abundances with LTE and NLTE calculations.

### 3.1. Atmospheric Parameters

#### 3.1.1. Reddening Estimates

While interstellar reddening  $E(B - V)$  affects estimates of effective temperatures based on color indices, it has been usually assumed that no reddening corrections need be applied to the stars within 100 pc. However, this assumption could break down for some stars, with significant reddening ( $\gtrsim 0.01$  mag), even if they are within 100 pc, because the maps of reddening in the Galaxy show a very patchy distribution of reddening at all galactic latitudes (Burstein & Heiles 1978, 1982). Because  $E(B - V) = 0.10$  mag has been found to alter the derived  $T_{\text{eff}}$  by 400 – 550 K for such cool stars as in our sample (Laird, Carney, & Latham 1988),  $E(B - V) = 0.01$  may change  $T_{\text{eff}}$  by 40 – 55 K. Our test calculations confirmed these changes in  $T_{\text{eff}}$ . Consequently, we decided to estimate  $E(B - V)$  for *all* our sample stars regardless of their distances.

Almost all reddening corrections had been made based on the maps of Burstein & Heiles (1978, 1982) until 1998 when a new, modern source of reddening was published by Schlegel, Finkbeiner, & Davis (1998). They constructed the full-sky maps of the Galactic dust using the far-infrared data observed by the *Infrared Astronomy Satellite (IRAS)* and the Diffuse Infrared Background Experiment (DIRBE) on board the *COBE* satellite. They demonstrated that the new dust maps predict reddening with an accuracy of 16 %, which is twice as accurate as that estimated from the Burstein & Heiles' maps in regions of low and moderate reddening. Hence we used the new dust maps of Schlegel et al. (1998) to estimate  $E(B - V)$  of our sample stars. After we estimated a total reddening  $E(B - V)_T$  in

the direction of a given star, the  $E(B - V)$  to the star at distance  $D$  pc was calculated with the same relation as employed by Beers et al. (2000),  $E(B - V) = E(B - V)_T \{1 - \exp[-|D \sin b|/h]\}$ , where  $b$  is the Galactic latitude and  $h$  is a scale height of 125 pc assumed for the dust layer. Distances were estimated from the *Hipparcos* parallaxes  $\pi$  listed in Table 1. Resulting  $E(B - V)$  larger than 0.01 mag are given in the fifth column of Table 1 and used for determinations of  $T_{\text{eff}}$  and  $\log g$ .

As clearly seen from these results, reddening should be examined for stars even at close distances. Note a typical example of HD 190248 at a distance of  $D = 6.11$  pc ( $\pi = 163.73$  mas) with a reddening of  $E(B - V) = 0.02$  mag in the François ' (1987) sample.

### 3.1.2. Effective Temperatures

Effective temperatures of the HIRES sample, one giant star HD 111721, and one dwarf star HD 182572 were derived using the empirical calibration of Alonso, Arribas, & Martínez-Roger (1999a) for  $(V - K)$  index and [Fe/H], which is based on the infrared flux method (IRFM). The observed  $(V - K)$  indices for these 8 stars were figured out by adopting  $K$  magnitudes from Alonso, Arribas, & Martínez-Roger (1994) for HD 44007, HD 84937, HD 111721, and HD 182572, from Alonso, Arribas, & Martínez-Roger (1998) for HD 88609, HD 165195, and HD 184266, and from Carney (1983) for HD 175305. Resulting values are given in Table 1. These  $(V - K)$  indices were corrected for reddening using a standard relation,  $E(V - K) = 2.72E(B - V)$ , and applied to the empirical calibration. With regard to one more parameter [Fe/H] in the empirical calibration, we adopted the values where the second decimal place is rounded off to 5 or 0, and listed them in the fourth column of Table 2. The original values for these [Fe/H] are presented in the eleventh column of Table 1 together with the literature entered in the last column.

Effective temperatures of the OAO, François (1987, 1988), and Clegg et al. (1981) sample stars were estimated using the IRFM-based empirical calibration (Eq. 9) of Alonso, Arribas, & Martínez-Roger (1996b) for Strömgren ( $b - y$ ) and  $c_1$  indices and [Fe/H]. The Strömgren indices were adopted from Hauck and Mermilliod (1998) and listed in the ninth and tenth columns of Table 1. We used the rounded-off values of [Fe/H] the same as the case of HIRES sample. Reddening corrections were applied to these Strömgren indices making use of the adopted  $E(B - V)$  and the well known relations of  $E(b - y) = 0.73E(B - V)$  and  $E(c_1) = 0.15E(B - V)$  (Crawford 1973).

The resulting  $T_{\text{eff}}$  for all our sample stars are rounded off to the second digit (10 K) and summarized in the second column of Table 2. The  $T_{\text{eff}}$  determined by Alonso et al. (1999b) and Alonso et al. (1996a) for giants and dwarfs, respectively, are listed in the sixth column for comparison. The differences  $\delta T_{\text{eff}} = T_{\text{eff}} \text{ (Ours)} - T_{\text{eff}} \text{ (Alonso et al's)}$  are also given in the seventh column. Inspection of  $\delta T_{\text{eff}}$  demonstrates that our  $T_{\text{eff}}$  values agree well with those of Alonso et al mostly to within  $\pm 100$  K, while discrepancies larger than 100 K are found in five stars. This good agreement is reasonably expected since both our and the Alonso et al's  $T_{\text{eff}}$  are based on the same IRFM framework.

### 3.1.3. Surface Gravities

Surface gravities ( $\log g$ ) were derived following the standard procedures, based on data of  $T_{\text{eff}}$ ,  $V$  magnitude, parallax,  $E(B - V)$ , bolometric magnitude, and the theoretical evolutionary track.

First, we calculated the absolute visual magnitudes ( $M_V$ ) from data of  $V$  and *Hipparcos* parallaxes ( $\pi$ ) adopting a  $V$ -band absorption  $A_V = 3.1E(B - V)$ . We then separately estimated bolometric corrections of  $V$ ,  $BC(V)$ , for giants and dwarfs. The  $BC(V)$  for giants

were calculated for  $T_{\text{eff}}$  and [Fe/H] adopted in Table 2 using the Alonso et al.’s (1999a) calibrations (Eq. 17 or 18) which are presented as a function of  $T_{\text{eff}}$  and [Fe/H]. On the other hand, BC( $V$ ) for dwarfs were obtained for  $T_{\text{eff}}$  and [Fe/H] adopted, interpolating the grid of BC( $V$ ) for  $\log g = 4.0$  models calculated by Alonso, Arribas, & Martínez-Roger (1995). Resulting BC( $V$ ) were applied to estimate of absolute bolometric magnitudes  $M_{\text{bol}}$  which are listed in Table 1.

The masses of stars were evaluated for the adopted  $T_{\text{eff}}$  and  $M_{\text{bol}}$  on the theoretical evolutionary tracks of the Italian group. For the sample of giants and the very metal-poor dwarf HD 84937, we adopted the evolutionary tracks with solar-scaled mixture of abundances and initial chemical compositions computed by Girardi et al. (1996:  $[Y = 0.230, Z = 0.0001]$  track for HD 84937, 88609, and 165195) and Girardi et al. (2000:  $[Y = 0.23, Z = 0.0004]$  for HD 44007 and 184266;  $[Y = 0.23, Z = 0.001]$  for HD 111721 and 175305). In the estimates for the masses of HD 44007 and HD 165195, we failed to find the evolutionary tracks corresponding to the positions with  $T_{\text{eff}}$  and  $M_{\text{bol}}$  on the HR diagram, so we assumed  $0.6 M_{\odot}$  for these two stars. This assumption is probably adequate since a mass range indicated from masses obtained for our sample of remaining giants is  $0.6 – 1.0 M_{\odot}$ .

For the sample of remaining dwarfs, the masses were inferred on the theoretical evolutionary tracks computed by Salasnich et al. (2000). We used their evolutionary tracks with  $\alpha$ -enhanced mixture of abundances and initial chemical compositions of  $[Y = 0.250, Z = 0.008]$ ,  $[Y = 0.273, Z = 0.019]$ , and  $[Y = 0.320, Z = 0.04]$  for our sample stars with  $[\text{Fe}/\text{H}] < -0.1$ ,  $-0.1 \leq [\text{Fe}/\text{H}] \leq +0.1$ , and  $[\text{Fe}/\text{H}] > +0.1$ , respectively.

In these procedures of  $\log g$  estimate, we adopted the following values for the Sun:  $T_{\text{eff},\odot} = 5780$  K,  $\log g_{\odot} = 4.44$ , and  $M_{\text{bol},\odot} = 4.74$ . The  $\log g$  values thus derived are summarized in the third column of Table 2.

### 3.1.4. *Microturbulences*

Microturbulences ( $\xi$ ) of the stars in the HIRES sample were determined based on  $W_\lambda$  data of Fe I lines measured in Paper I, eliminating any trend of abundances with line strength. The values of  $\xi$  for all samples of dwarfs were calculated using the empirical relation,

$$\xi \text{ (km s}^{-1}\text{)} = 1.25 + 8 \times 10^{-4}(T_{\text{eff}} - 6000) - 1.3(\log g - 4.5),$$

which was found by Edvardsson et al. (1993). As for the  $\xi$  of the giant star HD 111721, it was taken from Ryan & Lambert (1995) because this relation cannot be applied for giants. Resulting values of  $\xi$  are listed in the fifth column of Table 2.

## 3.2. LTE Analyses

We used the WIDTH9 program written by R. L. Kurucz to determine the LTE abundances of S and Fe based on the adopted model atmospheres.

### 3.2.1. *Fe Abundances*

The Fe abundances of the HIRES sample were derived from both Fe I and Fe II lines by analyzing their  $W_\lambda$  given in Paper I, while those of the OAO and François (1987, 1988) samples were obtained from the measured  $W_\lambda$  of selected Fe I lines. The  $gf$  values compiled by Kurucz (1995) were used. The enhancement factor,  $f_6$ , which should be multiplied by the classical van der Waals damping constant, was estimated to be 1.2 for Fe I lines with lower excitation potentials ( $\chi$ ) less than 2.6 eV using the empirical calibration by Simmons & Blackwell (1982), and  $f_6 = 1.4$  was adopted from Edvardsson et al. (1993) for lines with

$\chi > 2.6$  eV.

The results of Fe abundances yielded from the HIRES sample are presented in Table 6 as  $[\text{Fe I}/\text{H}]_{\text{LTE}}$  and  $[\text{Fe II}/\text{H}]_{\text{LTE}}$ , which were calculated relative to the solar value of  $\log \text{Fe}_\odot = 7.51$  (Holweger, Kock, & Bard 1995). Hereafter, we will separately deal with the abundances obtained from Fe I and Fe II lines for the HIRES sample.

Resulting Fe abundances of the OAO and François (1987, 1988) samples are summarized in Table 3 together with  $W_\lambda$ , the  $gf$  values, and the lower excitation potentials ( $\chi$ ). The averages of  $\log \text{Fe}$  are also listed as  $\log \text{Fe}_{\text{ILTE}}$  in Table 7. The values of  $[\text{Fe I}/\text{H}]_{\text{LTE}}$  of the OAO sample were calculated relative to our solar value of  $\log \text{Fe}_\odot = 7.41$  to eliminate the systematic errors due to uncertainties of the  $\log gf$  and  $f_6$  values, while those of the François (1987, 1988) sample relative to  $\log \text{Fe}_\odot = 7.51$ . Those of Clegg et al. (1981) were simply adopted from the values analyzed by them and are listed in Table 7. The  $[\text{Fe I}/\text{H}]_{\text{LTE}}$  of the giant star HD 111721 is included in Table 6.

### 3.2.2. S Abundances

The S abundances ( $\log S$ ) were calculated adopting the  $gf$  values compiled by Kurucz (1995):  $\log gf = +0.080$  for the 8694.641 Å line and  $\log gf = -0.510$  for the 8693.958 Å line. The lower excitation potential for both lines is  $\chi = 7.87$  eV, which means that the S I lines analyzed are high excitation lines and so the abundances derived from them are sensitive to errors of  $T_{\text{eff}}$  rather than  $\log g$  especially when the lines are considerably weaker ( $\lesssim 20$  mÅ) and  $T_{\text{eff}}$  is cooler than about 5500 K. The enhancement factor  $f_6 = 2.5$  was adopted from Feltzing & Gonzalez (2001).

The  $\log S$  of the OAO sample stars were derived from  $W_\lambda$  of the blended S I line feature which is regarded as one line, and are shown in the last column of Table 4 and also in

Table 7 as  $\log S_{\text{LTE}}$ . The S abundances of the HIRES sample and the samples of François (1987, 1988) and Clegg et al. (1981) were obtained from the two S I lines, and are listed in Table 5. The averaged abundances for the samples of François (1987, 1988) and Clegg et al. (1981) are also given in Table 7 as  $\log S_{\text{LTE}}$ .

The values of  $[\text{S}/\text{H}]_{\text{LTE}}$  for the HIRES sample and the samples of François (1987, 1988) and Clegg et al. (1981) were calculated relative to the solar value of  $\log S_{\odot} = 7.21$  (Anders & Grevesse 1989), while those of the OAO sample were calculated relative to our solar value of  $\log S_{\odot} = 7.22$ . These results are listed in Tables 6 and 7 for the HIRES sample and the giant star HD 111721 and for all the remaining dwarfs, respectively.

The synthetic line profiles of S I lines at 8693.9 Å and 8694.6 Å were computed for the HIRES sample stars using the adopted S abundances, and overplotted in Figures 1a – 1f. Except for the upper limit case of HD 88609, the synthetic profiles of S I 8694.6 Å line for the remaining stars fit well with the observed ones, while the observed profile of HD 84937 (Figure 1b) slightly disagrees with the synthetic one on the blue side of the profile which seems asymmetric relative to the synthetic one. The line profile of this star may be influenced by a rather low S/N ratio ( $\sim 230$ ) and incomplete removal of the fringe pattern. Although we confidently regard the absorption feature at 8694.6 Å observed in HD 84937 as the S I line, we should confirm the line with a follow-up observation.

### 3.2.3. $[\text{S}/\text{Fe}]$

The values of  $[\text{S}/\text{Fe}]$  for the HIRES sample were computed from the above-obtained  $[\text{Fe I}/\text{H}]_{\text{LTE}}$ ,  $[\text{Fe II}/\text{H}]_{\text{LTE}}$ , and  $[\text{S}/\text{H}]_{\text{LTE}}$ , and are given as  $[\text{S}/\text{Fe I}]_{\text{LTE}}$  and  $[\text{S}/\text{Fe II}]_{\text{LTE}}$  in the fifth and sixth columns of Table 6, respectively, together with the  $[\text{S}/\text{Fe I}]_{\text{LTE}}$  of the giant star HD 111721. The error bars are discussed in §3.4.

In Table 7, the  $[S/Fe\,I]_{LTE}$  results are listed in the sixth column for the dwarf samples of OAO, François (1987, 1988), and Clegg et al. (1981).

### 3.3. NLTE Analyses

The NLTE abundances of S were computed for the two S I lines following the same procedures as described in Takada-Hidai & Takeda (1996). The grids of NLTE corrections were constructed for the parameter ranges of  $T_{\text{eff}} = 4500 - 6500$  K,  $\log g = 1.0 - 5.0$ , and  $[\text{Fe}/\text{H}] = 0.0 - -3.0$ , assuming a constant microturbulence of  $2.0 \text{ km s}^{-1}$  and changing enhancement of S abundances. The grids for S I 8693.9 and S I 8694.6 lines are presented in Tables A1 and A2 in the Appendix, respectively. The NLTE corrections for the S abundance defined as  $\Delta(S) \equiv \log S_{\text{NLTE}} - \log S_{\text{LTE}}$  were evaluated on these grids for two S I lines of the HIRES sample and the samples of François (1987, 1988) and Clegg et al. (1981) using their measured  $W_{\lambda}$ . As for the OAO sample, since the S I lines are blended, we computed the  $W_{\lambda}$  of each S I line corresponding to the derived  $\log S_{\text{LTE}}$  and used them to estimate  $\Delta(S)$ . The average values of each  $\Delta(S)$  are given in the seventh column of Tables 6 and 7 for the HIRES sample and the giant star HD 111721 and for the sample of dwarfs, respectively.

The NLTE abundances of Fe were calculated for  $[\text{Fe I/H}]_{LTE}$  in all our samples using the polynomial relation derived by Israelian et al. (2001), which is based on the NLTE work of Thévenin & Idiart (1999). The results are shown as  $[\text{Fe I/H}]_{NLTE}$  in Tables 6 and 7.

The values of  $[S/Fe\,I]_{NLTE}$  were computed based on the above-obtained  $[S/H]_{LTE}$ ,  $\Delta(S)$ , and  $[\text{Fe I/H}]_{NLTE}$ , and are summarized in Tables 6 and 7 for each sample.

Since Fe abundances inferred from Fe II lines are separately dealt with in the HIRES sample, the results of  $[S/Fe\,II]_{NLTE}$  are also entered in Table 6. Here we applied the values

of  $[\text{Fe II}/\text{H}]_{\text{LTE}}$  to those of  $[\text{S}/\text{H}]_{\text{NLTE}}$  to get these results because an LTE Fe abundance deduced from Fe II has been found to be free from NLTE effects and reliable enough as suggested, for example, by Lambert et al. (1996) in their abundance study of RR Lyrae stars and by Thévenin & Idiart (1999) and Gratton et al. (1999) in studies of the NLTE effect on Fe II in metal-poor stars.

### 3.4. Error Analyses

Although there are many factors which yield errors in the abundances, we focus only on the main factors of uncertainties of  $T_{\text{eff}}$  ,  $\log g$  , and  $\xi$ .

The uncertainties of  $T_{\text{eff}}$  for all our samples were estimated to be  $\Delta T_{\text{eff}} = \pm 100$  K, taking into account the  $T_{\text{eff}}$  differences ( $\delta T_{\text{eff}}$  ) shown in Table 2, since most of our  $T_{\text{eff}}$  values agree well with those of Alonso et al. (1996a, 1999b) within  $\pm 100$  K.

The uncertainties of  $\log g$  are mainly caused by errors in  $T_{\text{eff}}$  , stellar mass, and  $M_{\text{bol}}$ . Test calculations have found that  $\Delta T_{\text{eff}} = 100$  K corresponds to  $\Delta \log g \sim 0.06$  dex. Errors in the mass are introduced from a selection of theoretical evolutionary tracks for fixed  $T_{\text{eff}}$  and  $M_{\text{bol}}$  (i.e. luminosity). Mass errors of  $\sim 0.05 M_{\odot}$  estimated on the evolutionary tracks corresponds to  $\Delta \log g \sim 0.05$  dex. Errors of  $M_{\text{bol}}$  essentially come from the parallax errors. The typical error of 3 % for the parallax yields  $\Delta \log g \sim 0.06$  dex. The quadratic sum of these uncertainties in  $\log g$  amounts to  $\pm 0.1$  dex. Allowing 0.05 dex for other possible error sources in the estimation procedures, we simply added this value to the quadratic sum and adopted  $\Delta \log g = \pm 0.15$  dex as the total uncertainty.

The uncertainties of microturbulences  $\xi$  for the HIRES sample were deduced from test calculations to examine whether Fe I abundances show any trend with line strength for different values of  $\xi$ . Since  $\xi$  for the samples of OAO, François , and Clegg et al. were

estimated using the empirical relation of Edvardsson et al. (1993), the uncertainty of  $\Delta\xi \simeq 0.22 \text{ km s}^{-1}$  was estimated for the above uncertainties of  $T_{\text{eff}}$  and  $\log g$ . The rms scatter for this relation was suggested to be about  $0.3 \text{ km s}^{-1}$  by Edvardsson et al. (1993), so that the total uncertainty became  $\pm 0.37 \text{ km s}^{-1}$ . We then adopted  $\Delta\xi = \pm 0.5 \text{ km s}^{-1}$  as the total uncertainty allowing for other possible errors.

The abundance errors of S and Fe for the HIRES sample and HD 111721 were calculated for these uncertainties, and are given in Table 6 as the error bars on the [S/Fe] values. The abundance errors for the remaining dwarfs sample were also evaluated and listed in Table 8. We regard the combined error of  $\pm 0.16 \text{ dex}$  as a typical error for [S/Fe I] values in the sample of dwarfs.

#### 4. Results and Discussion

The results of abundance analyses of S and Fe are summarized in Tables 6 and 7 for six stars of the HIRES sample and the giant star HD 111721 and for 61 dwarfs, including the Sun, respectively. Since nine stars of the OAO sample overlap with those of the samples of François (1987, 1988; four stars) and Clegg et al. (1981; five stars), the abundance results of the OAO sample were preferentially adopted for these stars. We will describe these results below and discuss the results for S and Fe abundances of all our samples.

##### 4.1. NLTE Corrections

While the NLTE corrections of the S abundances,  $\Delta(S)$ , are found to be in the range of  $-0.09 - 0.00 \text{ dex}$  for all of our sample, most of them concentrate on the range of  $-0.01 - -0.03 \text{ dex}$ . Consequently, neglect of NLTE effect does not produce significant errors leading to the wrong conclusions of behavior of S. On the other hand, as seen from the comparison

of  $[\text{Fe I/H}]_{\text{LTE}}$  with  $[\text{Fe I/H}]_{\text{NLTE}}$ , NLTE corrections of Fe I abundances are found to be considerably larger with the range of  $-0.09 - +0.29$  dex. The negative correction values in the range of  $-0.09 - -0.02$  dex are assigned only to the nine metal-rich stars, but all positive ones are for our sample of metal-poor stars, which distribute mostly in the range of  $+0.05 - +0.15$  dex and  $+0.20 - +0.29$  dex among the samples of dwarfs and giants, respectively. These NLTE corrections for Fe I abundance yield significant changes in  $[\text{S/Fe I}]$ , so that they should be examined when we investigate the behavior of  $[\text{S/Fe I}]$  against  $[\text{Fe I/H}]$ . However, we should note that Gratton et al. (1999) computed NLTE corrections of Fe I abundances for dwarfs ( $\log g = 4.5$ ) and low gravity ( $\log g = 1.5$  and  $2.25$ ) stars in the metallicity range of  $-3 - 0$  dex, and concluded that NLTE corrections are very small (mostly  $< 0.05$  dex) in dwarfs of  $T_{\text{eff}}$  less than 7000 K, while those in low gravity stars are less than 0.4 dex for  $T_{\text{eff}} < 6000$  K and the metallicity range of  $-1 - -3$  dex. Using their Figure 9, NLTE corrections for our giants sample were estimated to be less than about 0.15 dex, which are systematically smaller than those adopted in this study. Since  $[\text{Fe/H}]$  values of cool metal-poor stars are mainly determined from Fe I lines, further examinations of NLTE effect on Fe I abundance are worth performing.

As mentioned in section §3.3, the abundances derived from Fe II lines can be regarded as being reliably free from NLTE effects. Hence analyses of Fe II lines are recommended whenever such data are available.

#### 4.2. Behavior of $[\text{S/Fe}]$

To clarify the behavior of S in the metallicity range  $-3 \lesssim [\text{Fe/H}] \lesssim +0.5$ , we plotted  $[\text{S/Fe}]_{\text{LTE}}$  and  $[\text{S/Fe}]_{\text{NLTE}}$  against  $[\text{Fe/H}]_{\text{LTE}}$  and  $[\text{Fe/H}]_{\text{NLTE}}$  in Figures 2 and 3, respectively.

We first deal with the LTE behavior of  $[\text{S/Fe}]$  shown in Figure 2. As for  $[\text{S/Fe I}]$  in

all our samples of dwarfs and giants, it shows an increasing trend as  $[\text{Fe I}/\text{H}]$  decreases. A slope of this trend is calculated to be  $-0.27 \pm 0.15$  (where  $\pm 0.15$  are  $1\sigma$  errors, and these errors are also given to the slopes yielded from a least-square linear fit in other cases) by a least-square linear fit for all the  $[\text{S}/\text{Fe I}]$  results derived from the atmospheric models adopted in this study, except for an upper limit of HD 88609. The upper limit results of HD 88609 are not considered for the least-square linear fits in both cases of LTE and NLTE. This linear fit gives  $[\text{S}/\text{Fe I}] \sim 0.7$  at  $[\text{Fe I}/\text{H}] = -2.5$ , while  $[\text{S}/\text{Fe I}] \sim 1.2$  dex of HD 165195 deviates from the fit by about 0.5 dex around the same metallicity. The high value of HD 165195 seems to occur from the adopted  $T_{\text{eff}}$  of 4190 K which is on the lowest boundary of a range of  $T_{\text{eff}}$  (4131 – 4507 K) previously determined (see Paper I). This low  $T_{\text{eff}}$  produces the high S abundance derived from high-excitation lines and the lower Fe I abundance which breaks ionization equilibrium between Fe I and Fe II by a factor of 0.5 dex. Our test calculations showed that  $\log g$  should be lowered by about 0.5 to obtain ionization equilibrium between Fe I and Fe II with abundance differences of 0.3 dex. However, such low value of  $\log g \sim 0.5$  may not be valid since it is inferred from the mass of  $\sim 0.2M_{\odot}$ , which seems unreasonable for HD 165195, when  $T_{\text{eff}}$  and  $M_{\text{bol}}$  are fixed. If we calculate the  $[\text{S}/\text{Fe I}]$  value based on the atmospheric model determined by Pilachowsky et al. (1996) and adopted in Paper I, this results in  $+0.58 \pm 0.28$  dex as listed in the Pap.I entry of Table 6, and plotted with a filled asterisk in Figure 2. Adopting this Pap.I result of  $[\text{S}/\text{Fe I}]$ , a least-square linear fit yields a slope of  $-0.23 \pm 0.13$ , which is almost the same as the above-obtained slope of  $-0.27$ .

The  $[\text{S}/\text{Fe II}]$  values of the HIRES sample are also plotted in Figure 2 with half-filled diamond. In a case of HD 165195, the value listed in the Pap.I entry of Table 6 is also plotted with an open asterisk, which is located very close to the point inferred from this study (the Ours entry of Table 6). Combining these HIRES data with the  $[\text{S}/\text{Fe I}]$  data of OAO, François (1987, 1988), and Clegg et al. (1981), it is found that  $[\text{S}/\text{Fe}]$  shows a

continuous increase with a slope of  $-0.23 \pm 0.13$  as  $[\text{Fe}/\text{H}]$  decreases. This trend supports the one found in the case of  $[\text{S}/\text{Fe I}]$ .

Now, we inspect the NLTE behavior of  $[\text{S}/\text{Fe}]$  depicted in Figure 3. Because the NLTE analysis seems to be more reliable than the LTE one, we preferentially adopt the NLTE results as our final results in this study. As concerns  $[\text{S}/\text{Fe I}]$  of all our dwarfs and giants samples, it shows the same trend as in the above LTE case. However, since significant NLTE corrections to  $\text{Fe I}$  abundances make  $\text{Fe I}$  abundances of metal-poor stars higher and  $[\text{S}/\text{Fe I}]$  lower, the slope becomes  $-0.17 \pm 0.15$ , which is flatter than the LTE case, as illustrated by the least-square linear fit drawn in Figure 3 with dashed line. If we consider the  $[\text{S}/\text{Fe II}]$  values of the HIRES sample together with  $[\text{S}/\text{Fe I}]$  data of OAO, François (1987, 1988), and Clegg et al. (1981), we find a slope of  $-0.19 \pm 0.14$ . Both slopes remain almost unchanged for the  $[\text{S}/\text{Fe}]$  points in the Pap.I entry of Table 6 for the case of HD 165195.

Judging from the trends of LTE and NLTE behaviors of  $[\text{S}/\text{Fe}]$  against  $[\text{Fe}/\text{H}]$  observed in all our sample stars, we may safely conclude that  $[\text{S}/\text{Fe}]$  increases progressively and continuously with a slope of  $\sim -0.2$  as  $[\text{Fe}/\text{H}]$  decreases from  $+0.5$  dex to  $-3$  dex, though the observed data are distributed with a range of scatter of  $0.3 - 0.5$  dex. Our conclusion is qualitatively consistent with that of Israelian & Rebolo (2001). They found that  $[\text{S}/\text{Fe}]$  shows an increase trend with the slope of  $-0.46 \pm 0.06$  which is roughly twice as steep as those found in our sample stars. If we combine the results of six stars observed by Israelian & Rebolo (2001) with those of our samples and calculate the slope of increase trend of  $[\text{S}/\text{Fe I}]$ , we obtain the slope of  $-0.25 \pm 0.17$ , which is significant at the  $1.5 \sigma$  level. This least-square linear fit is depicted with solid line in Figure 3, together with Israelian & Rebolo's (2001) data plotted with a double circle. The same slope of  $-0.25 \pm 0.15$ , which is significant at the  $1.7 \sigma$  level, is also derived from the combination of data of Israelian

& Rebolo (2001) and our data which include the results of [S/Fe II] instead of [S/Fe I] in the HIRES sample. Although this slope,  $-0.25$ , of the trend is significant only at the  $1.5 - 1.7 \sigma$  level and still flatter than that of Israelian & Rebolo (2001), it is more favorable to our above conclusion. As for a steeper slope found by Israelian & Rebolo (2001), which is significant at the  $7.7 \sigma$  level, it might be influenced by a bias in a smaller number of their sample (26 stars in their Figure 3) in comparison with our sample of 67 stars [73 stars in our Figure 3, including 6 stars of Israelian & Rebolo (2001)]. A slope is essentially determined by [S/Fe] in halo stars, so that further observations of a larger sample of halo stars are indispensable to establish an increase trend of [S/Fe] with a trustworthy value of slope. It is also interesting that the slope of  $-0.25$  is comparable to those ( $\sim -0.3$ ) found for [O/Fe] (e.g. Paper I; Israelian et al. 2001). As discussed below, since O and S are volatile elements, it may be plausible to expect that they show a similar behavior against metallicity, [Fe/H].

On the contrary, the linearly increasing trend of [S/Fe] is not consistent with the conclusion suggested by François (1988) that [S/Fe] forms a plateau in halo stars. His conclusion seems to be affected by a bias in that his sample does not contain halo stars with  $[\text{Fe}/\text{H}] \lesssim -1.5$ .

Now, we briefly discuss our results in relation with the theoretical studies of chemical evolution of the Galaxy. Theoretical predictions based on standard SNe II and Ia models may not explain our linearly increasing trend of [S/Fe] in the range of  $[\text{Fe}/\text{H}] \lesssim -1$  (e.g. Chiappini et al. 1999; Goswami & Prantzos 2000), however, it may be possible to explain the observed trend of [S/Fe] if we consider the explosive nucleosynthesis in “hypernovae”, i.e., SNe with very large explosion energies of  $E = (10 - 100) \times 10^{51}$  ergs, proposed by Nomoto et al. (2001) and studied in detail by Nakamura et al. (2001). Nakamura et al. (2001) carried out detailed nucleosynthesis calculations for hypernovae with these energies as well as for ordinary core-collapse SNe with  $E = 1 \times 10^{51}$  ergs for comparison. They

found that a larger amount of S is synthesized by oxygen burning in hypernovae, which leads to higher [S/Fe] ratios to be observed in metal-poor halo stars if hypernovae occurred in the early phase of the Galaxy evolution. For example, inspection of Table 2 or 3 of Nakamura et al. (2001) suggests that the ratios of  $[S/Fe] \gtrsim 1$  may be attained in the ejecta of hypernovae with  $E \gtrsim 10^{52}$  ergs in the metallicity range of  $[Fe/H] < -1$ . They also found that even one hypernova can produce 2–10 times more Fe than normal core-collapse SNe, which makes  $[\alpha\text{-elements}/Fe]$  ratios smaller. Consequently, if such metal-poor halo stars, as included in our sample, formed from some hypernova ejecta, the iron mass of these stars should be smaller by factors of  $\gtrsim 10$  than those presented, for instance, in Table 2 to explain the [S/Fe] trend observed in this study and Israeli & Rebolo (2001). As discussed for the case of abundances in the black hole binary GRO J1655–40 by Nakamura et al. (2001), there may be some possible ways to produce the ejecta with smaller Fe mass using hypernova models with a certain mass cut at large  $M_r$  (mass included in the radius  $r$  of the precollapse star) or with asymmetric explosions such as have a jet. In addition to these possibilities, the mixing and dilution of ejecta to the interstellar medium plays an important role in determining the metallicity of halo stars. Nakamura et al. (1999) suggested that the [Fe/H] of halo stars are mainly determined by the mass of interstellar hydrogen mixed with the ejecta of the relevant SN II, and that the mass of such interstellar hydrogen varies by an order of magnitude and is larger for both cases of the larger explosion energy of SN and the larger Strömgren radius of the progenitor. A more detailed discussion on the justification of the increasing trend of [S/Fe] has been made with relation to hypernovae/supernovae by Israeli & Rebolo (2001).

Another possible explanation for the increasing trend of [S/Fe] at low [Fe/H] has been proposed by Ramaty et al. (2000) and Ramaty, Lingenfelter, & Kozlovsky (2000) in connection with their explanation of a similar increasing trend of [O/Fe] (cf. Israeli et al. 2001). Taking into account the delayed deposition of the SN products into the interstellar

medium due to differences in transport and mixing, which are inferred from the different characteristics of volatile (O) and refractory (Fe) elements with dust grains, they simulated the evolution of  $[O/Fe]$  versus  $[Fe/H]$  for the case of a short mixing delay time (1 Myr) for O and a longer one (30 Myr) for Fe. They found that  $[O/Fe]$  should increase monotonically up to  $\sim 1$  at  $[Fe/H] \sim -3$  with a slope consistent with the previously observed one (eg. Israelian et al. 2001), and then predicted that the similar trend should be observed for another volatile element of S, which is just the demonstrated case in this study.

## 5. Conclusions

LTE and NLTE abundances of sulfur in 6 metal-poor giants and 61 dwarfs (62 dwarfs, including the Sun) were explored in the range of  $-3 \lesssim [Fe/H] \lesssim +0.5$  using S I 8693.9 Å and 8694.6 Å lines. NLTE effects in the S abundances are found to be small and practically negligible. The behavior of  $[S/Fe]$  vs.  $[Fe/H]$  exhibits a linearly increasing trend without plateau with decreasing  $[Fe/H]$ . Although the slope of the linearly increasing trend is found to be in the range of  $-0.17 - -0.25$  for the NLTE behavior, the value of  $-0.25$  is the most favorable one for all observed data used in this study. It is interesting to note that this slope is comparable to that ( $\sim -0.3$ ) observed in  $[O/Fe]$ , which may be plausible since S and O are both volatile elements.

The observed behavior of S may require chemical evolution models of the Galaxy, in which scenarios of hypernovae nucleosynthesis and/or time-delayed deposition into interstellar medium are incorporated.

Since our conclusions are essentially based on the small sample of halo stars, further observations should be performed for a larger sample of halo stars to establish our conclusions and explore the behavior of S in the very beginning stage of the chemical

evolution of the Galaxy.

We would like to thank G. Israelian for his helpful comments and discussions, and the referees, S. G. Ryan and P. François , for their comments which helped us to improve the paper. We also wish to thank D. J. Schlegel and T. C. Beers for their kind help with handling of the dust maps, J. X. Prochaska and M. Asplund for the comments, and K. Osada for his great help with revision of atmospheric parameters.

We are grateful to the staff of the Okayama Astrophysical Observatory and the W. M. Keck Observatory for their help with observations. One of us (MTH) acknowledges the financial supports from grant-in-aid for the scientific research (A-2, No. 10044103) by Japan Society for the Promotion of Science as well as from Tokai University in 1999 fiscal year, which enabled his observation with HIRES.

This work is partially supported from grant-in-aid for the scientific research by Japan Society for the Promotion of Science for MTH (C-2, No. 13640246).

This research has made use of the SIMBAD database, operated at CDS, Strasbourg, France.

## A. Appendix

The results of NLTE calculations for two S I lines at 8693.9 Å and 8694.6 Å are given in Tables A1 and A2, respectively.

The meanings of each column are as follows:

1. The 1st column: Code stands for models with coded atmospheric parameters of  $T_{\text{eff}}$  ,  $\log g$  , and metallicity. For example, *t65g50m0* stands for a model with  $T_{\text{eff}} = 6500$  K,

$\log g = 5.0$ , and  $[\text{Fe}/\text{H}] = 0.0$ ;  $t50g40m2$  a model with  $T_{\text{eff}} = 5000$  K,  $\log g = 4.0$ , and  $[\text{Fe}/\text{H}] = -2.0$ .

2. The 2nd column:  $\lambda$  is the wavelength of the S I line.
3. The 3rd column:  $\xi$  is the microturbulence.
4. The 4th column:  $[\text{S}/\text{Fe}]_i$  stands for the input value of  $[\text{S}/\text{Fe}]$  corresponding to  $A_{\text{input}}$  of S. The solar value of Fe adopted is 7.51.
5. The 5th column:  $A_{\text{input}}$  is the input value of S abundance for theoretical calculations of equivalent widths with LTE and NLTE.
6. The 6th column:  $W(\text{LTE})$  is the theoretical LTE equivalent widths calculated with  $A_{\text{input}}$ .
7. The 7th column:  $W(\text{NLTE})$  is the theoretical NLTE equivalent widths calculated with  $A_{\text{input}}$ .
8. The 8th column:  $A(\text{NLTE})$  is the abundance of S calculated from  $W(\text{NLTE})$  under the assumption of NLTE. Although  $A(\text{NLTE})$  should be equal to  $A_{\text{input}}$  in the strict sense, there are practically small (and negligible) discrepancy due to numerical problems in computation.
9. The 9th column:  $A(\text{LTE})$  is the abundance of S calculated from  $W(\text{NLTE})$  under the assumption of LTE.
10. The 10th column:  $\Delta$  is the NLTE correction defined as  $\Delta \equiv A(\text{NLTE}) - A(\text{LTE})$ .

## REFERENCES

Abia, C., Rebolo, R., Beckman, J. E., & Crivellari, L. 1988, *A&A*, 206, 100

Alonso, A., Arribas, S., & Martínez-Roger, C. 1994, *A&AS*, 107, 365

Alonso, A., Arribas, S., & Martínez-Roger, C. 1995, *A&A*, 297, 197

Alonso, A., Arribas, S., & Martínez-Roger, C. 1996a, *A&AS*, 117, 227

Alonso, A., Arribas, S., & Martínez-Roger, C. 1996b, *A&A*, 313, 873

Alonso, A., Arribas, S., & Martínez-Roger, C. 1998, *A&AS*, 131, 209

Alonso, A., Arribas, S., & Martínez-Roger, C. 1999a, *A&AS*, 140, 261

Alonso, A., Arribas, S., & Martínez-Roger, C. 1999b, *A&AS*, 139, 335

Anders, E., & Grevesse, N. 1989, *Geochim. Cosmochim. Acta*, 53, 197

Axer, M., Fuhrmann, K., & Gehren, T. 1994, *A&A*, 291, 895

Balachandran, S. 1990, *ApJ*, 354, 310

Barbuy, B. 1988, *A&A*, 191, 121

Beers, T. C., Chiba, M., Yoshii, Y., Platais, I., Hanson, R. B., Fuchs, B., & Rossi, S. 2000, *AJ*, 119, 2866

Boesgaard, A. M., King, J. R., Deliyannis, C. P., & Vogt, S. S. 1999, *AJ*, 117, 492

Branch, D., & Bell, R. A. 1971, *MNRAS*, 153, 57

Burkhart, C., & Coupry, M. F. 1991, *A&A*, 249, 205

Burstein, D., & Heiles, C. 1978, *ApJ*, 225, 40

Burstein, D., & Heiles, C. 1982, AJ, 87, 1165

Carney, B. W. 1983, AJ, 88, 610

Carretta, E., Gratton, R. G., & Sneden, C. 2000, A&A, 356, 238

Chiappini, C., Matteucci, F., Beers, T.C., & Nomoto, K. 1999, ApJ, 515, 226

Clegg, R. E. S., Lambert, D. L., & Tomkin, J. 1981, ApJ, 250, 262

Crawford, D. L. 1973, IAU Symp. 54, Interstellar Dust and Related Topics, ed. J. M. Greenberg & H. C. van de Hulst (Dordrecht: D. Reidel Publ. Co.), 93

Edvardsson, B., Andersen, J., Gustafsson, B., Lambert, D. L., Nissen, P. E., & Tomkin, J. 1993, A&A, 275, 101

Feltzing, S., & Gonzalez, G. 2001, A&A, 367, 253

François, P. 1986, A&A, 165, 183

François, P. 1987, A&A, 176, 294

François, P. 1988, A&A, 195, 226

Fulbright, J. P., & Kraft, R. P. 1999, ApJ, 118, 527

Girardi, L., Bressan, A., Bertelli, G., & Chiosi, C. 2000, A&AS, 141, 371

Girardi, L., Bressan, A., Chiosi, C., Bertelli, G., & Nasi, E. 1996, A&AS, 117, 113

Goswami, A., & Prantzos, N. 2000, A&A, 359, 191

Gratton, R. G., Carretta, E., Eriksson, K., & Gustafsson, B. 1999, A&A, 350, 955

Gratton, R. G., & Sneden, C. 1994, A&A, 287, 927

Hauck, B., & Mermilliod, M. 1998, A&AS, 129, 431

Holweger, H., Kock, M., & Bard, A. 1995, A&A, 296, 233

Israelian, G., & Rebolo, R. 2001, ApJ, 557, L43

Israelian, G., Rebolo, R., García López, R. J., Bonifacio, P., Molaro, P., Basri, G., & Shchukina, N. 2001, ApJ, 551, 833

Johnson, D. J., Friedlander, M. W., & Katz, J. I. 1993, ApJ, 407, 699

Kuroczkin, D., & Wiszniewski, A. 1977, Acta Astron., 27, 145

Kurucz, R. L. 1993, Kurucz CD-ROM No.13 (Harvard-Smithsonian Center for Astrophysics)

Kurucz, R. L. 1995, Kurucz CD-ROM No.23 (Harvard-Smithsonian Center for Astrophysics)

Laird, J. B., Carney, B. W., & Latham, D. W. 1988, AJ, 95, 1843

Lambert, D. L., Heath, J. E., Lemke, M., & Drake, J. 1966, ApJS, 103, 183

McWilliam, A. 1990, ApJS, 74, 1075

McWilliam, A. 1997, ARA&A, 35, 503

Nakamura, T., Umeda, H., Iwamoto, K., Nomoto, K., Hashimoto, M., Raphael Hix, W., & Thielemann, F. 2001, ApJ, 555, 880

Nakamura, T., Umeda, H., Nomoto, K., Thielemann, F., & Burrows, A. 1999, ApJ, 517, 193

Nomoto, K., Mazzali, P. A., Nakamura, T., Iwamoto, K., Maeda, K., Suzuki, T., Turatto, M., Danziger, I. J., & Patat, F. 2001, in Supernovae and Gamma Ray Bursts, ed. K. Sahu, M. Livio, & N. Pagagia (Cambridge: Cambridge Univ. Press), in press (astro-ph/0003077)

Oinas, V. 1974, *ApJS*, 27, 405

Pasquini, L., Liu, Q., & Pallavicini, R. 1994, *A&A*, 287, 191

Perryman, M. A. C. et al. 1997, The Main Hipparcos Catalogue, ESA

Peterson, R. C. 1978, *ApJ*, 224, 595

Pilachowski, C. A., Sneden, C., & Kraft, R. P. 1966, *AJ*, 111, 1689

Prochaska, J. X., Naumov, S. O., Carney, B. W., McWilliam, A., & Wolfe, A. 2000, *AJ*, 120, 2513

Ramaty, R., Lingenfelter, R. E., & Kozlovsky, B. 2000, in IAU Symp. 198, The Light Elements and Their Evolution, ed. L. da Silva, M. Spite, & J. R. de Medeiros (San Francisco: ASP), 51

Ramaty, R., Scully, S. T., Lingenfelter, R. E., & Kozlovsky, B. 2000, *ApJ*, 534, 747

Ryan, S. G., & Lambert, D. L. 1995, *AJ*, 109, 2068

Sadakane, K., Honda, S., Kawanomoto, S., Takeda, Y., & Takada-Hidai, M. 1999, *PASJ*, 51, 505

Salasnich, B., Girardi, L., Weiss, A., & Chiosi, C. 2000, *A&A*, 361, 1023

Schlegel, D. J., Finkbeiner, D. P., & Davis, M. 1998, *ApJ*, 500, 525

Simmons, G. J., & Blackwell, D. E. 1982, *A&A*, 112, 209

Spite, M., Pasquini, L., & Spite, F. 1994, *A&A*, 290, 217

Spite, M., & Spite, F. 1973, *A&A*, 23, 63

Takada-Hidai, M., & Takeda, Y. 1996, *PASJ*, 48, 739

Takeda, Y., Takada-Hidai, M., Sato, S., Sargent, W. S. W., Lu, L., Barlow, T. A., & Jugaku, J. 2002, ApJ submitted (astro-ph/0007007) (Paper I)

Thévenin, F., & Idiart, I. P. 1999, ApJ, 521, 753

Timmes, F. X., Woosley, S. E., & Weaver, T. A. 1995, ApJS, 98, 617

Vogt, S. S. 1994, Proc. SPIE, 2198, 362

### Figure Captions

Fig. 1a. — Observed and synthetic spectra in the vicinity of two S I lines for HD 44007, where observed data are shown by filled circles, and synthetic spectrum computed using the adopted LTE S abundance is overplotted with solid line.

Fig. 1b. — The same as Fig.1a, but for HD 84937.

Fig. 1c. — The same as Fig.1a, but for HD 88609.

Fig. 1d. — The same as Fig.1a, but for HD 165195.

Fig. 1e. — The same as Fig.1a, but for HD 175305

Fig. 1f. — The same as Fig.1a, but for HD 184266.

Fig. 2. — Behavior of sulfur with respect to iron in LTE results. The results of [S/Fe I] and [S/Fe II] calculated for HD 165195 using the model atmosphere adopted in Paper I are plotted with filled and open asterisks, respectively.

Fig. 3. — Behavior of sulfur with respect to iron in the NLTE results. The results of [S/Fe I] and [S/Fe II] calculated for HD 165195 using the model atmosphere adopted in Paper I are plotted the same as Figure 2. The least-square linear fit with a slope of  $-0.17$  obtained for [S/Fe I] results of all our samples of dwarfs and giants is illustrated by dashed line, while the same fit with a slope of  $-0.25$  is shown by solid line, which is derived from [S/Fe I] data of all our samples together with those of Israelian & Rebolo (2001) plotted with double circle.

TABLE 1  
BASIC DATA OF SAMPLE STARS

HD	HR	Sp.Typ	$\pi$ (mas)	$E(B - V)$	$V$	$M_{\text{bol}}$	$V - K$	$b - y$	$c_1$	[Fe/H]	Ref <sup>a</sup>
Giants											
44007	...	G5IV:w	5.17	0.07	8.05	1.08	2.36	0.559	0.364	-1.57	1
88609	...	G5IIIw	0.63	0.01	8.59	-2.92	2.54	0.683	0.564	-2.72	1
165195	...	K3p	2.20	0.10	7.31	-1.97	3.29	0.919	0.723	-2.05	1
175305	...	G5III	6.18	0.05	7.18	0.74	2.08	0.504	0.290	-1.33	1
184266	...	F2V	3.28	0.07	7.59	-0.22	1.78	0.425	0.611	-1.57	1
François (1988) sample:											
111721	...	G6V	3.29	0.04	7.97	0.16	2.18	0.512	0.300	-1.34	10
Dwarfs											
HIRES sample:											
84937	...	sdF5	12.44	0.02	8.33	3.55	1.25	0.302	0.369	-2.17	1
OAO sample:											
3795	173	G3/G5V	35.02	0.00	6.14	3.62	...	0.447	0.295	-0.73	2
6582	321	G5Vb	132.42	0.00	5.17	5.54	...	0.437	0.213	-0.86	3
13555	646	F5V	33.19	0.02	5.23	2.70	...	0.303	0.468	-0.32	4
14412	683	G5V	78.80	0.00	6.33	5.58	...	0.442	0.236	-0.53	2
15335	720	G0V	32.48	0.01	5.89	3.30	...	0.383	0.360	-0.22	4
17948	860	F4V	37.78	0.01	5.59	3.37	...	0.290	0.444	-0.29	5
18768	...	F8	21.65	0.01	6.72	3.21	...	0.388	0.330	-0.62	4
22484	1101	F9IV-V	72.89	0.01	4.29	3.46	...	0.367	0.376	-0.11	4
33256	1673	F2V	39.99	0.01	5.11	3.01	...	0.299	0.442	-0.30	4
37495	1935	F4V	23.54	0.00	5.28	2.06	...	0.312	0.500	-0.11	6
40136	2085	F1V	66.47	0.01	3.71	2.76	...	0.218	0.622	-0.05	7
49933	2530	F2V	33.45	0.00	5.78	3.31	...	0.270	0.460	-0.43	4
59984	2883	F5V	33.40	0.00	5.90	3.39	...	0.356	0.336	-0.87	2
60532	2906	F6V	38.91	0.00	4.44	2.29	...	0.336	0.468	-0.18	4
62301	...	F8V	29.22	0.01	6.74	3.92	...	0.362	0.310	-0.69	4
69897	3262	F6V	55.17	0.00	5.13	3.75	...	0.315	0.384	-0.26	4
76932	3578	F7/8IV/V	46.90	0.01	5.80	4.00	...	0.359	0.299	-0.82	4
142860	5933	F6IV	89.92	0.00	3.85	3.53	...	0.319	0.401	-0.16	4
165908	6775	F7V	63.88	0.00	5.05	3.92	...	0.356	0.322	-0.62	3
182572	7373	G8IV	66.01	0.01	5.17	4.07	1.68	...	...	0.15	8
201891	...	F8V-VI	28.26	0.01	7.37	4.43	...	0.358	0.262	-0.98	3
207978	8354	F6IV-V	36.15	0.01	5.52	3.18	...	0.299	0.425	-0.53	3
216385	8697	F7IV	37.25	0.01	5.16	2.90	...	0.319	0.434	-0.25	4
217107	8734	G8IV	50.71	0.01	6.17	4.50	...	0.456	0.376	0.29	9
218470	8805	F5V	29.33	0.02	5.68	2.90	...	0.290	0.486	-0.13	4
François (1988) sample:											
24616	...	G8IV/V	15.87	0.01	6.68	2.31	...	0.521	0.318	-0.78	11
59984 <sup>b</sup>	2883	F5V	33.40	0.00	5.90	3.39	...	0.356	0.336	-0.87	2
63077	3018	G0V	65.79	0.01	5.36	4.25	...	0.377	0.278	-0.90	2
69897 <sup>b</sup>	3262	F6V	55.17	0.00	5.13	3.75	...	0.315	0.384	-0.26	4
94028	...	F4V	19.23	0.01	8.21	4.41	...	0.344	0.258	-1.51	11
104304	4587	G9IV	77.48	0.00	5.54	4.78	...	0.465	0.340	0.16	13
132475	...	F5/F6V	10.85	0.04	8.55	3.41	...	0.393	0.287	-1.48	11
148816	...	F8V	24.34	0.01	7.27	4.03	...	0.367	0.306	-0.74	4
157089	...	F9V	25.88	0.02	6.95	3.81	...	0.380	0.324	-0.59	4
193901	...	F7V	22.88	0.01	8.65	5.23	...	0.381	0.217	-0.98	3
201891 <sup>b</sup>	...	F8V-IV	28.26	0.01	7.37	4.43	...	0.358	0.262	-0.98	3
François (1987) sample:											
76932 <sup>b</sup>	3578	F7/F8IV/V	46.90	0.01	5.80	4.00	...	0.359	0.299	-0.82	4
88218	3992	F8V	32.55	0.01	6.14	3.51	...	0.397	0.355	-0.45	14
91324	4134	F6V	45.72	0.00	4.89	3.07	...	0.327	0.410	-0.43	12
102365	4523	G5V	108.23	0.00	4.89	4.88	...	0.410	0.278	-0.28	12
106516	4657	F5V	44.34	0.01	6.11	4.18	...	0.319	0.334	-0.70	15
114946	4995	G8III/IV	25.89	0.02	5.31	2.01	...	0.523	0.317	-0.24	12
121384	5236	G6IV-V	26.24	0.01	6.00	2.79	...	0.480	0.295	-0.45	12
136352	5699	G4V	68.70	0.00	5.65	4.66	...	0.403	0.297	-0.37	12
139211	5803	F6V	32.34	0.01	5.95	3.40	...	0.319	0.433	0.04	6
188376	7597	G5V	42.03	0.01	4.70	2.59	...	0.458	0.359	-0.13	14
190248	7665	G7IV	163.73	0.02	3.55	4.38	...	0.466	0.384	0.28	16
203608	8181	F6V	108.50	0.00	4.21	4.26	...	0.331	0.313	-0.60	3
211998	8515	A3V	30.00	0.00	5.29	2.40	...	0.448	0.235	-1.56	2

TABLE 1 (continued)

HD	HR	Sp.Typ	$\pi$ (mas)	$E(B - V)$	$V$	$M_{\text{bol}}$	$V - K$	$b - y$	$c_1$	[Fe/H]	Ref <sup>a</sup>
Clegg et al. (1981) sample:											
1461	72	G0V	42.67	0.01	6.47	4.46	...	0.420	0.362	0.23	17
4614	219	G0V	167.99	0.00	3.46	4.46	...	0.372	0.275	-0.31	4
6582 <sup>b</sup>	321	G5Vb	132.40	0.00	5.17	5.54	...	0.437	0.213	-0.86	3
10307	483	G1.5V	79.09	0.00	4.96	4.32	...	0.389	0.348	-0.02	4
16895	799	F7V	89.03	0.00	4.10	3.77	...	0.325	0.392	-0.02	4
30652	1543	F6V	124.60	0.00	3.19	3.61	...	0.298	0.415	0.02	18
33256 <sup>b</sup>	1673	F2V	39.99	0.01	5.11	3.01	...	0.299	0.442	-0.30	4
34411	1729	G1.5V	79.08	0.00	4.69	4.05	...	0.390	0.364	-0.30	4
63077	3018	G0V	65.79	0.01	5.36	4.25	...	0.377	0.278	-0.90	2
82328	3775	F6IV	74.15	0.00	3.17	2.43	...	0.314	0.463	-0.20	4
102870	4540	F9V	91.74	0.00	3.59	3.29	...	0.354	0.416	0.13	4
114710	4983	F9.5V	109.23	0.00	4.23	4.31	...	0.368	0.338	0.03	4
121370	5235	G0IV	88.17	0.00	2.68	2.32	...	0.374	0.488	0.19	4
128167	5447	F2V	64.66	0.00	4.47	3.44	...	0.254	0.480	-0.41	4
142860 <sup>b</sup>	5933	F6IV	89.92	0.00	3.85	3.53	...	0.319	0.401	-0.16	4
145675	...	K0V	55.11	0.00	6.61	5.01	...	0.537	0.438	0.31	19
185144	7462	K0V	173.41	0.00	4.67	5.60	...	0.472	0.267	-0.25	20
207978 <sup>b</sup>	8354	F6-V	36.15	0.01	5.52	3.18	...	0.299	0.425	-0.53	3
216385 <sup>b</sup>	8697	F7IV	37.25	0.01	5.16	2.90	...	0.319	0.434	-0.25	4
224930	9088	G5Vb	80.63	0.00	5.80	5.09	...	0.432	0.218	-0.86	3

<sup>a</sup> References to [Fe/H]

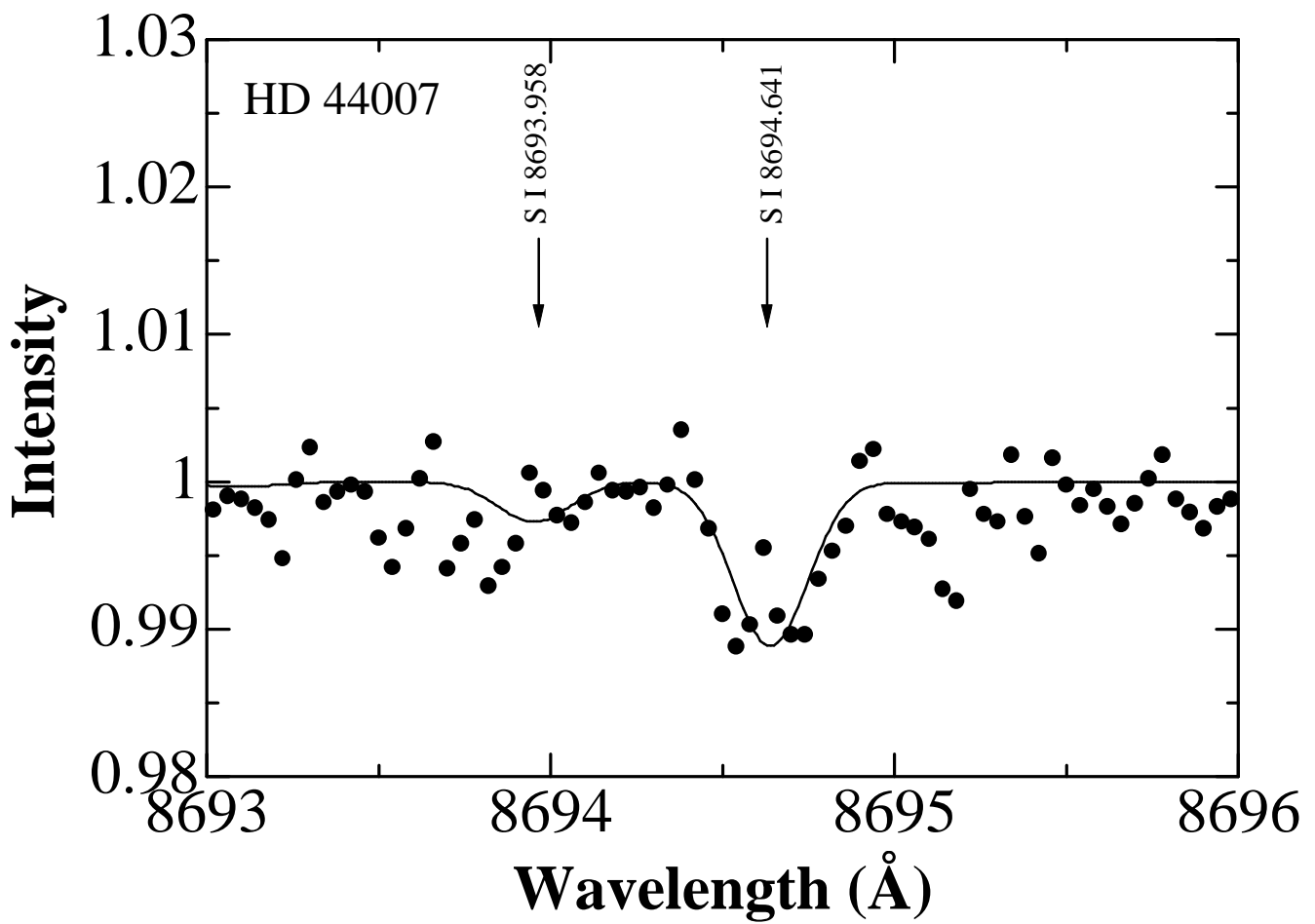
(1) Takeda et al. (2002), (2) Pasquini et al. (1994), (3) Axer et al. (1994), (4) Edvardsson et al. (1993), (5) Spite & Spite (1973), (6) Balachandran (1990), (7) Burkhart & Coupry (1991), (8) McWilliam (1990), (9) Sadakane et al. (1999), (10) Ryan & Lambert (1995), (11) Johnson et al. (1993), (12) Gratton & Sneden (1994), (13) François (1988), (14) François (1986), (15) Spite et al. (1994), (16) Abia et al. (1988), (17) Branch & Bell (1971), (18) Kuroczkin & Wiszniewski (1977), (19) Peterson (1978), (20) Oinas (1974)

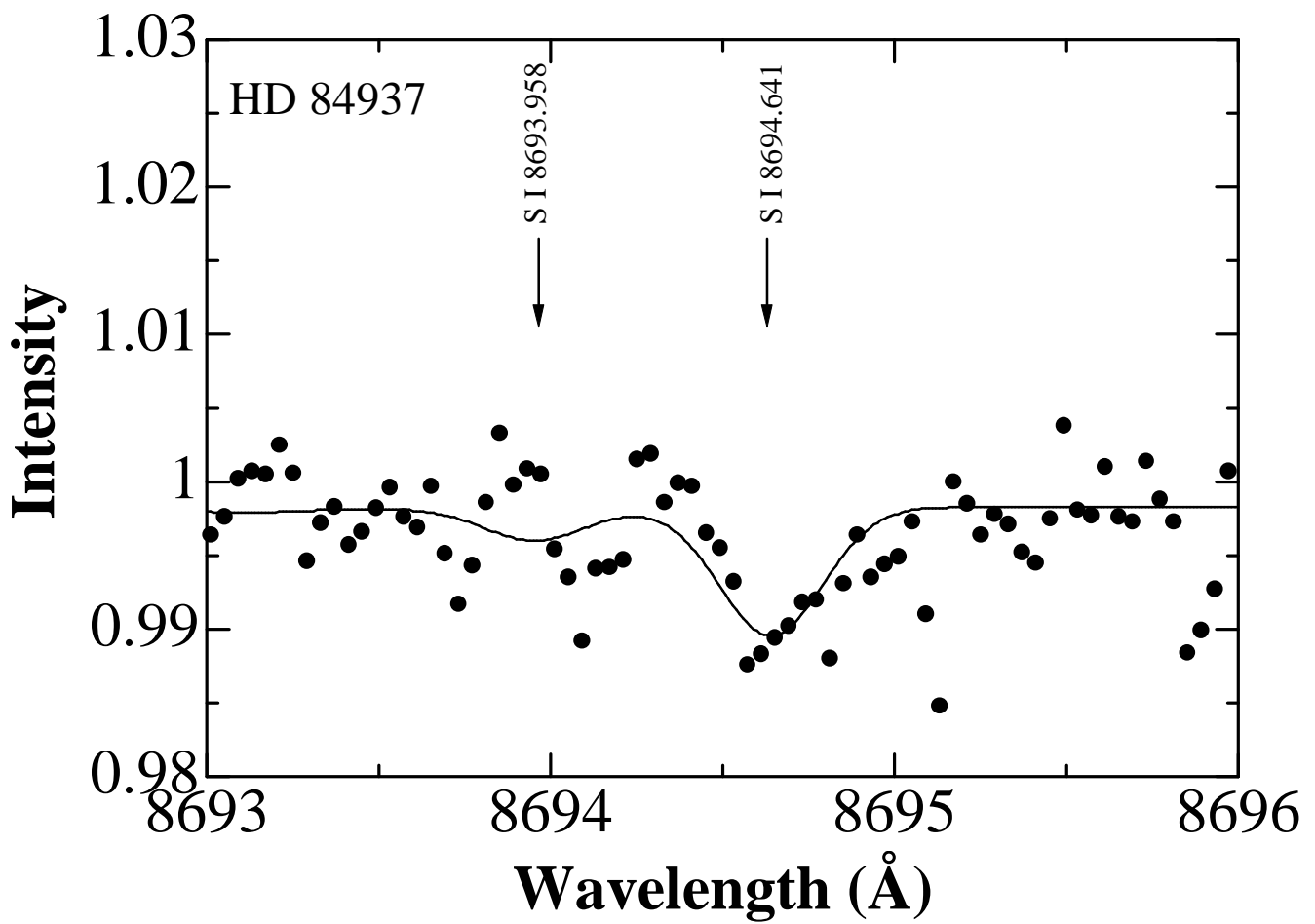
<sup>b</sup> Stars common to the OAO sample.

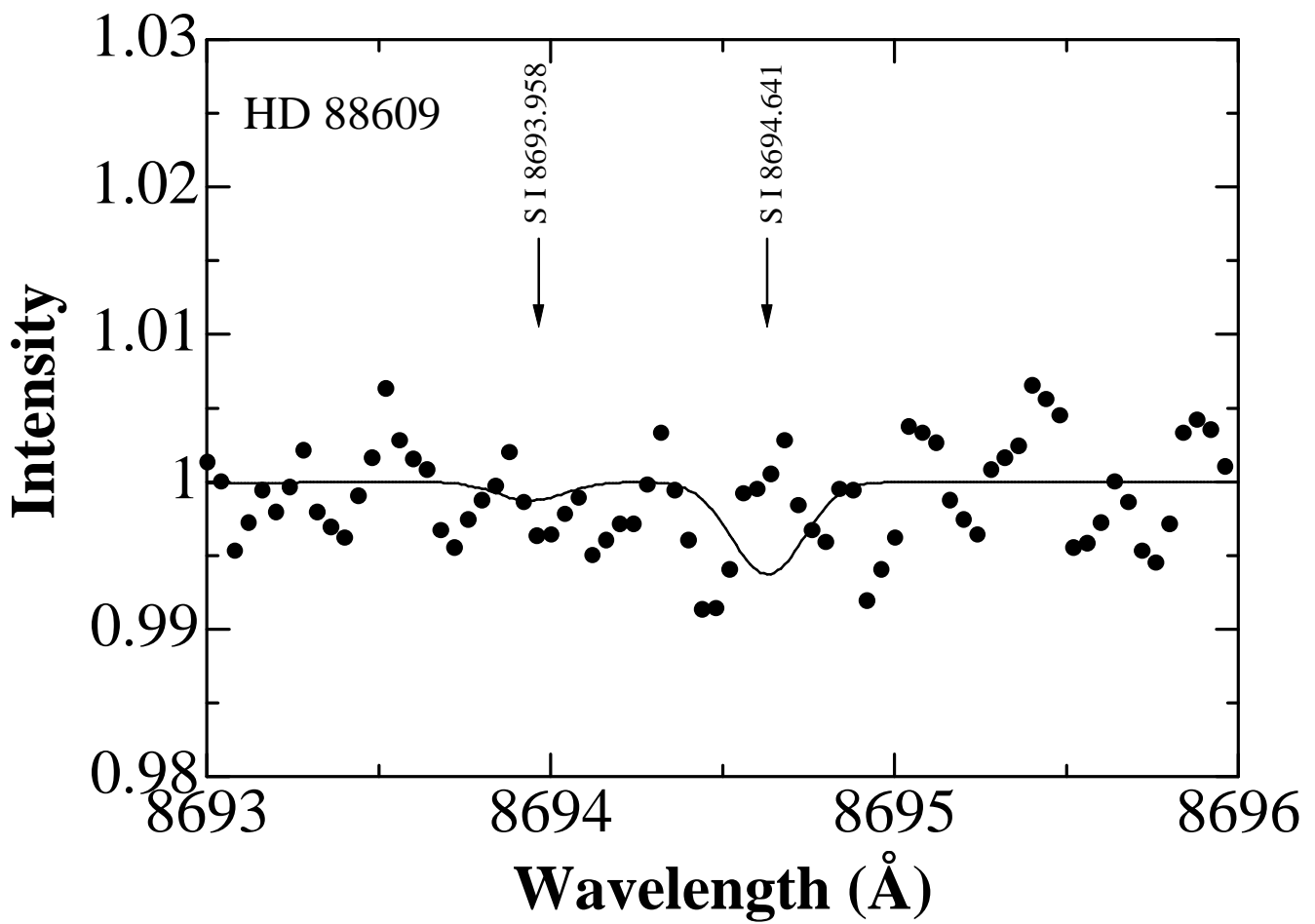
TABLE A1  
GRID OF NLTE CORRECTIONS FOR Si 8693.9 Å LINE

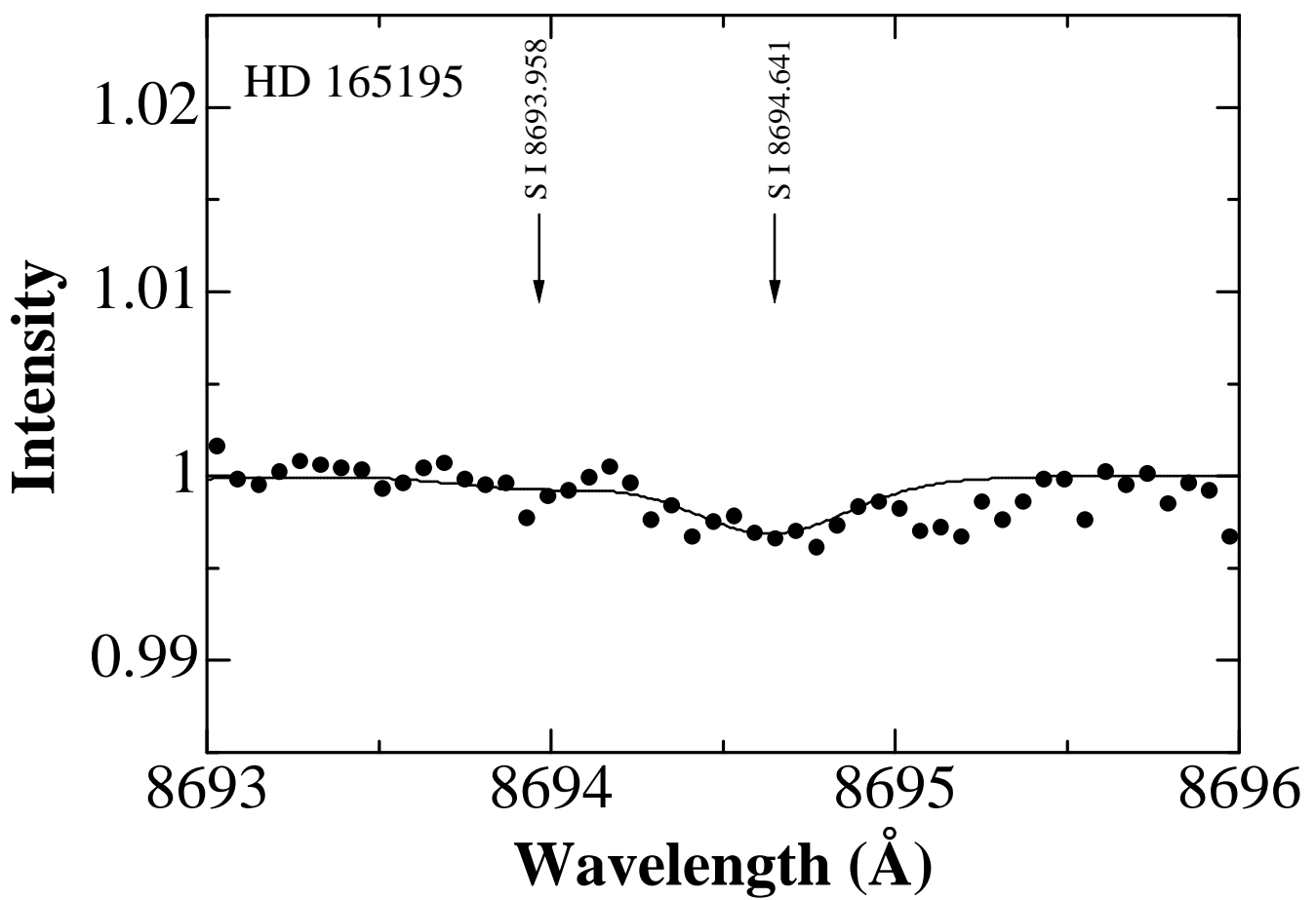
Code	$\lambda$ (Å)	$\xi$ (km s $^{-1}$ )	[S/Fe] $_{\text{i}}$	$A_{\text{input}}$	$W(\text{LTE})$ (mÅ)	$W(\text{NLTE})$ (mÅ)	$A(\text{NLTE})$	$A(\text{LTE})$	$\Delta$
t65g50m0	8693.93	2.0	-0.3	6.910	( 9.12)	9.12	6.914	6.921	-0.007
t65g50m0	8693.93	2.0	0.0	7.210	( 16.60)	16.98	7.215	7.222	-0.007
t65g50m0	8693.93	2.0	+0.3	7.510	( 28.84)	29.51	7.514	7.522	-0.008
t65g40m0	8693.93	2.0	-0.3	6.910	( 15.49)	16.60	6.913	6.942	-0.029
t65g40m0	8693.93	2.0	0.0	7.210	( 26.92)	28.18	7.205	7.242	-0.037
t65g40m0	8693.93	2.0	+0.3	7.510	( 42.66)	45.71	7.515	7.558	-0.043
t65g30m0	8693.93	2.0	-0.3	6.910	( 24.55)	28.18	6.912	6.998	-0.086
t65g30m0	8693.93	2.0	0.0	7.210	( 38.90)	45.71	7.210	7.319	-0.109
t65g30m0	8693.93	2.0	+0.3	7.510	( 58.88)	67.61	7.504	7.647	-0.143
t65g20m0	8693.93	2.0	-0.3	6.910	( 37.15)	45.71	6.904	7.048	-0.144
t65g20m0	8693.93	2.0	0.0	7.210	( 56.23)	70.79	7.214	7.420	-0.206
t65g20m0	8693.93	2.0	+0.3	7.510	( 77.62)	97.72	7.508	7.812	-0.304
t65g10m0	8693.93	2.0	-0.3	6.910	( 44.67)	57.54	6.914	7.096	-0.182
t65g10m0	8693.93	2.0	0.0	7.210	( 66.07)	85.11	7.208	7.476	-0.268
t65g10m0	8693.93	2.0	+0.3	7.510	( 87.10)	114.82	7.502	7.908	-0.406

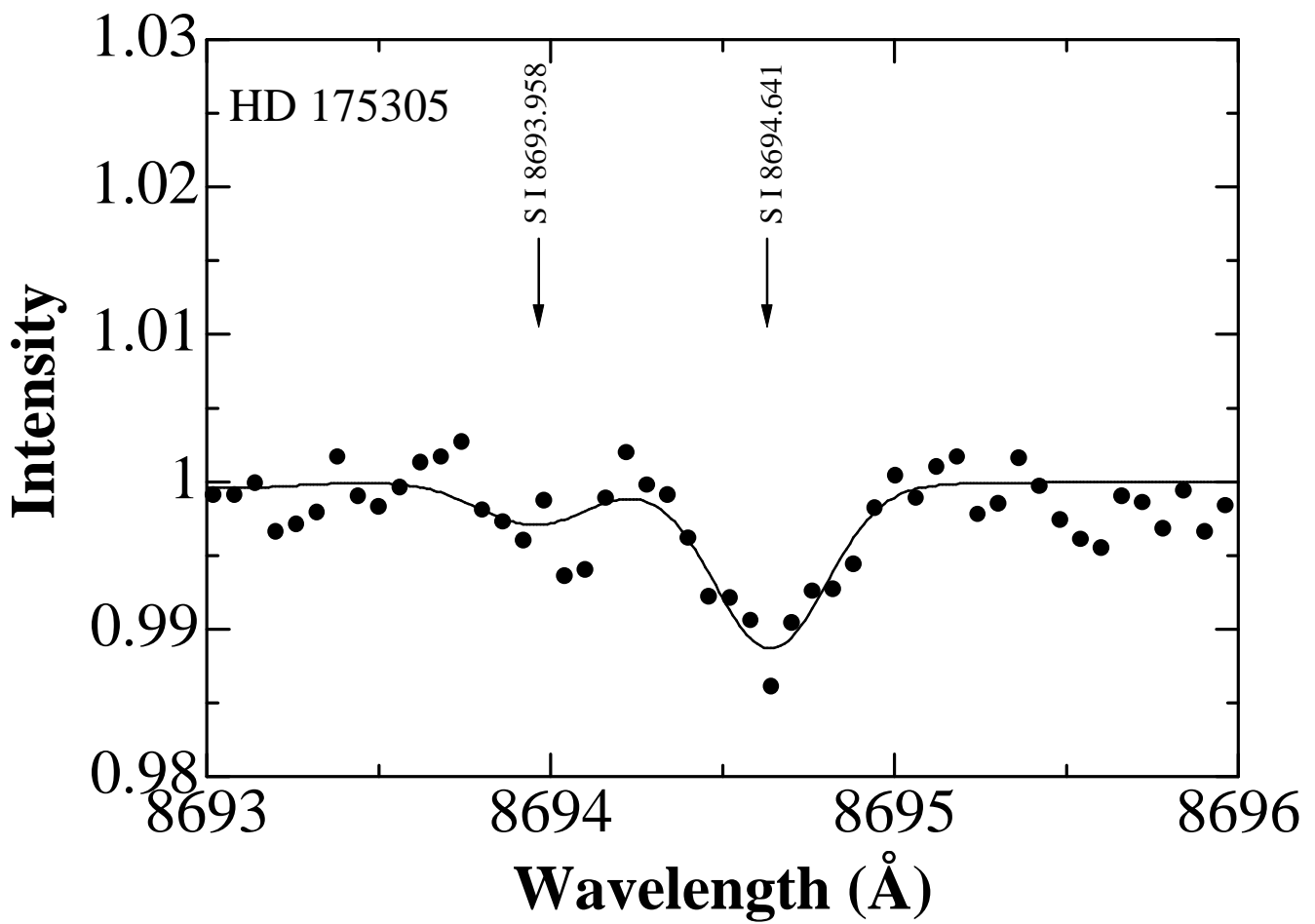
Note: This entire table is available only on-line as a machine-readable table.











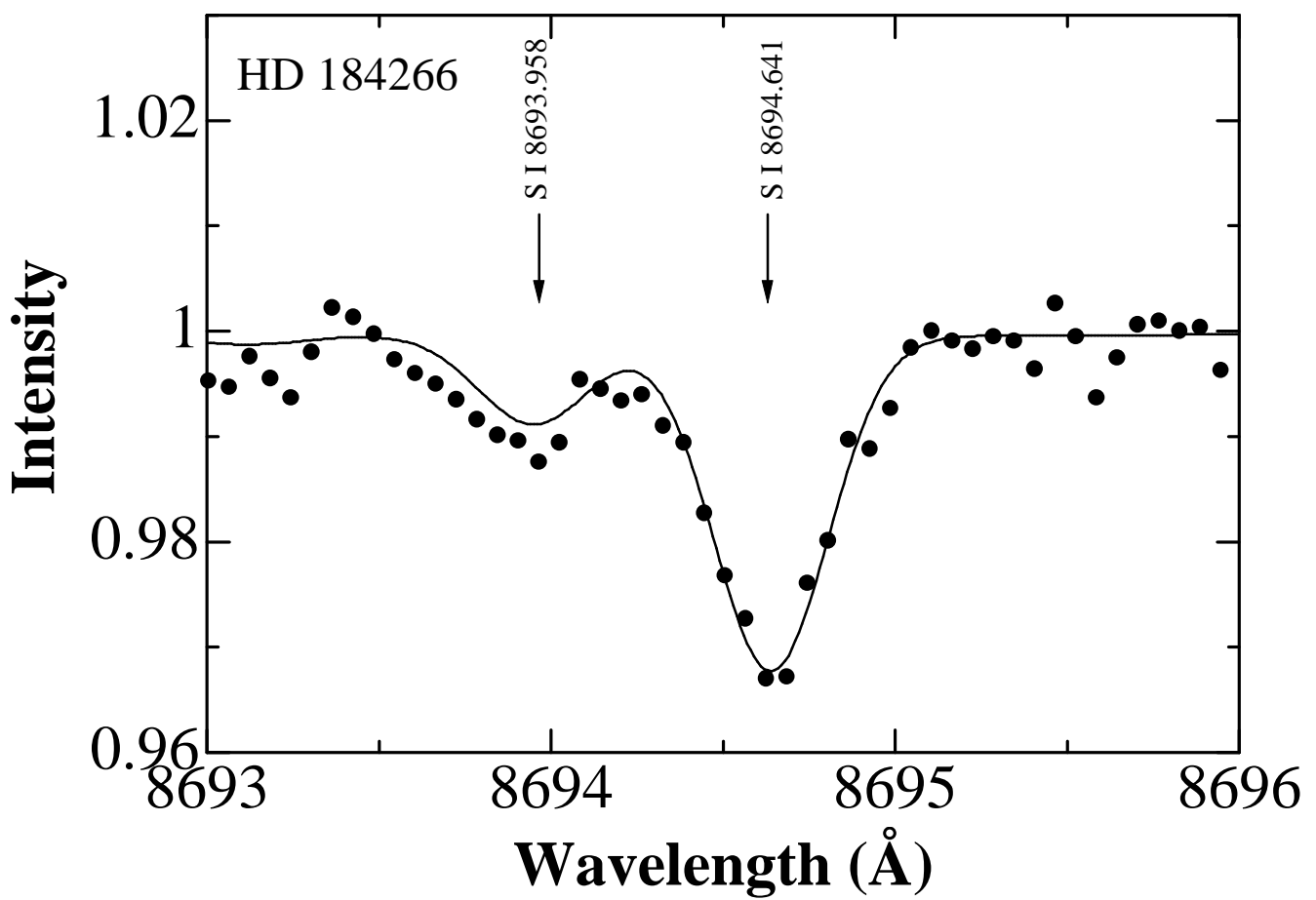


TABLE 2  
ADOPTED ATMOSPHERIC PARAMETERS

HD	$T_{\text{eff}}$	$\log g$	[Fe/H]	$\xi$ (km s $^{-1}$ )	$T_{\text{eff}}^{\alpha}$ (Alonso et al.'s)	$\delta T_{\text{eff}}$ (Ours - Alonso et al.'s)
Giants						
HIRES sample:						
44007	4910	2.47	-1.55	1.4	4851	+ 59
88609	4570	0.75	-2.70	1.9	4600	- 30
165195	4190	1.00	-2.05	1.3	4237	- 47
175305	5170	2.64	-1.35	1.5	5041	+ 129
184266	5640	2.17	-1.55	2.2	5587	+ 53
François (1988) sample:						
111721	5010	2.31	-1.35	1.2	...	...
Dwarfs						
HIRES sample:						
84937	6300	3.97	-2.15	1.1	6330	- 30
OAO sample:						
3795	5330	3.80	-0.75	1.6	...	...
6582	5340	4.42	-0.85	0.8	5315	+ 25
13555	6470	3.90	-0.30	2.4	...	...
14412	5340	4.44	-0.55	0.8	...	...
15335	5840	3.89	-0.20	1.9	...	...
17948	6500	4.13	-0.30	2.1	...	...
18768	5750	3.84	-0.60	1.9	...	...
22484	5960	4.02	-0.10	1.8	5998	- 38
33256	6440	3.99	-0.30	2.3	...	...
37495	6350	3.74	-0.10	2.5	...	...
40136	7190	4.15	-0.05	2.7	7013	+ 177
49933	6590	4.15	-0.45	2.2	6679	- 89
59984	5890	3.92	-0.85	1.9	5928	- 38
60532	6150	3.69	-0.20	2.4	...	...
62301	5900	4.09	-0.70	1.7	...	...
69897	6250	4.17	-0.25	1.9	6242	+ 8
76932	5900	4.12	-0.80	1.7	5727	+ 173
142860	6240	4.09	-0.15	2.0	6233	+ 7
165908	5900	4.09	-0.60	1.7	...	...
182572	5500	4.07	0.20	1.4	5518	- 18
201891	5880	4.25	-1.00	1.5	5909	- 29
207978	6400	4.03	-0.55	2.2	...	...
216385	6300	3.91	-0.25	2.3	...	...
217107	5490	4.15	0.30	1.3	...	...
218470	6600	4.01	-0.15	2.4	...	...
Sun	5780	4.44	0.00	1.2	5763	+ 17
François (1988) sample:						
24616	4980	3.08	-0.80	2.3	...	...
59984	5890	3.92	-0.85	1.9	5928	- 38
63077	5770	4.08	-0.90	1.6	...	...
69897	6250	4.17	-0.25	1.9	6242	+ 8
94028	5980	4.30	-1.50	1.5	6001	- 21
104304	5360	4.24	0.15	1.1	...	...
132475	5810	3.91	-1.50	1.9	5788	+ 22
148816	5860	4.11	-0.75	1.6	5851	+ 9
157089	5840	4.01	-0.60	1.8	5662	+ 178
193901	5710	4.52	-1.00	1.0	5750	- 40
201891	5880	4.25	-1.00	1.5	5909	- 29

TABLE 2 (continued)

HD	$T_{\text{eff}}$	$\log g$	[Fe/H]	$\xi$ (km s $^{-1}$ )	$T_{\text{eff}}^{\text{a}}$ (Alonso et al.'s)	$\delta T_{\text{eff}}$ (Ours – Alonso et al.'s)
François (1987) sample:						
76932	5900	4.12	−0.80	1.7	5727	+ 173
88218	5720	3.91	−0.45	1.8	...	...
91324	6150	3.92	−0.45	2.1	...	...
102365	5570	4.28	−0.30	1.2	...	...
106516	6200	4.31	−0.70	1.7	6208	− 8
114946	5060	3.07	−0.25	2.4	...	...
121384	5210	3.50	−0.45	1.9	...	...
136352	5620	4.22	−0.35	1.3	...	...
139211	6340	4.15	0.05	2.0	...	...
188376	5400	3.59	−0.15	2.0	...	...
190248	5480	4.16	0.30	1.3	...	...
203608	6070	4.27	−0.60	1.6	...	...
211998	5270	3.43	−1.55	2.1	...	...
Clegg et al. (1981) sample:						
1461	5690	4.28	0.25	1.3	5683	+ 7
4614	5810	4.23	−0.30	1.4	5817	− 7
6582	5340	4.42	−0.85	0.8	5315	+ 25
10307	5780	4.23	0.00	1.4	5874	− 94
16895	6220	4.23	0.00	1.8	...	...
30652	6430	4.25	0.00	1.9	6482	− 52
33256	6440	3.99	−0.30	2.3	...	...
34411	5790	4.14	0.05	1.6	5847	− 57
63077	5770	4.08	−0.90	1.6	...	...
82328	6300	3.78	−0.20	2.4	6338	− 38
102870	6010	3.94	−0.15	2.0	6095	− 85
114710	5920	4.29	0.05	1.5	5964	− 44
121370	5980	3.70	0.20	2.3	...	...
128167	6730	4.25	−0.40	2.2	6707	+ 23
142860	6240	4.09	−0.15	2.0	6233	+ 7
145675	5060	4.18	0.30	0.9	...	...
185144	5220	4.38	−0.25	0.8	5227	− 7
207978	6400	4.03	−0.55	2.2	...	...
216385	6300	3.91	−0.25	2.3	...	...
224930	5370	4.26	−0.85	1.1	...	...

<sup>a</sup> Adopted from Alonso et al. (1999b) and Alonso et al. (1996a) for giants and dwarfs, respectively.

TABLE A2  
GRID OF NLTE CORRECTIONS FOR Si 8694.6 Å LINE

Code	$\lambda$	$\xi$ (km s $^{-1}$ )	[S/Fe] $_{\text{i}}$	$A_{\text{input}}$	$W(\text{LTE})$ (mÅ)	$W(\text{NLTE})$ (mÅ)	$A(\text{NLTE})$	$A(\text{LTE})$	$\Delta$
t65g50m0	8694.63	2.0	-0.3	6.910	( 28.18)	28.84	6.910	6.918	-0.008
t65g50m0	8694.63	2.0	0.0	7.210	( 46.77)	46.77	7.206	7.216	-0.010
t65g50m0	8694.63	2.0	+0.3	7.510	( 70.79)	70.79	7.507	7.518	-0.011
t65g40m0	8694.63	2.0	-0.3	6.910	( 42.66)	44.67	6.908	6.950	-0.042
t65g40m0	8694.63	2.0	0.0	7.210	( 63.10)	66.07	7.206	7.268	-0.062
t65g40m0	8694.63	2.0	+0.3	7.510	( 85.11)	91.20	7.508	7.580	-0.072
t65g30m0	8694.63	2.0	-0.3	6.910	( 57.54)	67.61	6.913	7.057	-0.144
t65g30m0	8694.63	2.0	0.0	7.210	( 79.43)	93.33	7.211	7.408	-0.197
t65g30m0	8694.63	2.0	+0.3	7.510	( 100.00)	120.23	7.506	7.760	-0.254
t65g20m0	8694.63	2.0	-0.3	6.910	( 75.86)	97.72	6.916	7.209	-0.293
t65g20m0	8694.63	2.0	0.0	7.210	( 97.72)	125.89	7.205	7.614	-0.409
t65g20m0	8694.63	2.0	+0.3	7.510	( 120.23)	154.88	7.503	7.993	-0.490
t65g10m0	8694.63	2.0	-0.3	6.910	( 87.10)	114.82	6.910	7.309	-0.399
t65g10m0	8694.63	2.0	0.0	7.210	( 109.65)	144.54	7.200	7.710	-0.510
t65g10m0	8694.63	2.0	+0.3	7.510	( 128.82)	173.78	7.496	8.135	-0.639

Note: This entire table is available only on-line as a machine-readable table.

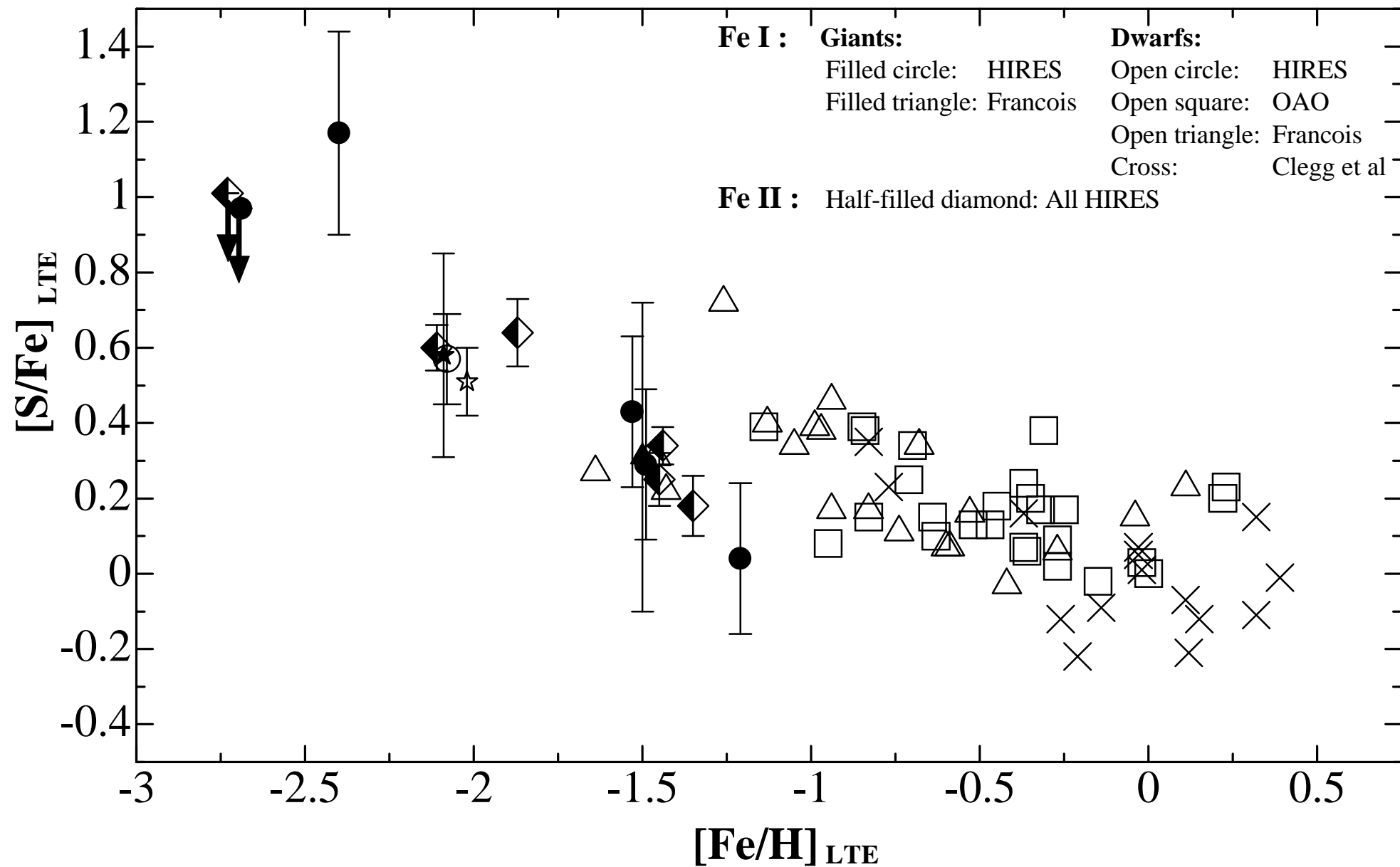


TABLE 3  
EQUIVALENT WIDTHS OF Fe I LINES AND LTE ABUNDANCES  
OF THE SAMPLES OF OAO AND FRANÇOIS (1987, 1988).

HD	$W_\lambda$ (mÅ) and $\log$ Fe $^a$							
	$\lambda$ (Å)	8582.271	8611.812	8621.618	8674.756	8688.642	8699.461	
	$\log g_f$	-1.993	-1.900	-2.024	-1.850	-1.212	-0.360	$\log$ Fe
	$\chi$ (eV)	2.990	2.845	2.949	2.832	2.176	4.956	(average)
OAO sample:								
3795	60.2	82.3	54.6	88.8	181.0	38.5		
	6.53	6.62	6.42	6.66	6.49	6.62	6.56	
6582	49.5	72.5	45.3	77.6	227.2	31.3		
	6.48	6.65	6.39	6.66	6.69	6.52	6.57	
13555	41.5	66.8	38.0	76.2	144.9	38.4		
	7.10	7.25	7.03	7.35	6.98	7.12	7.14	
14412	73.4	90.1	65.2	103.6	266.1	57.5		
	6.93	6.95	6.78	7.06	6.93	6.99	6.94	
15335	66.4	90.3	57.5	95.7	184.4	54.4		
	7.02	7.12	6.87	7.14	7.01	7.10	7.04	
17948	35.6	57.7	28.4	60.8	128.3	35.3		
	7.04	7.18	6.89	7.19	6.87	7.10	7.05	
18768	47.6	73.7	41.7	80.4	152.4	35.5		
	6.67	6.82	6.57	6.86	6.57	6.77	6.71	
22484	64.4	88.2	60.9	96.4	175.6	58.0		
	7.10	7.22	7.04	7.29	7.07	7.22	7.16	
33256	37.5	62.2	31.6	74.8	139.7	26.5		
	7.02	7.18	6.91	7.31	6.91	6.90	7.04	
37495	36.9: <sup>b</sup>	54.0: <sup>b</sup>	44.8: <sup>b</sup>	93.9: <sup>b</sup>	159.1	47.6: <sup>b</sup>		
	6.94:	6.98:	7.05:	7.44	6.97	7.21:	7.10	
40136	25.3 <sup>c</sup>	47.1	17.8: <sup>c</sup>	56.7	143.4	33.9: <sup>c</sup>		
	7.30	7.50	7.11:	7.64	7.44	7.36:	7.39	
49933	21.8 <sup>c</sup>	45.2	18.4 <sup>c</sup>	52.2	116.2	22.3 <sup>c</sup>		
	6.81	7.05	6.71	7.12	6.77	6.86	6.89	
59984	34.9	54.1	27.1	64.4	130.1	22.9		
	6.58	6.67	6.42	6.76	6.48	6.58	6.58	
60532	54.2	80.4	47.7	91.9	162.5	46.3		
	7.04	7.16	6.94	7.26	6.88	7.10	7.06	
62301	39.8	60.4	30.0:	69.4	143.5	25.3		
	6.69	6.80	6.50:	6.88	6.70	6.65	6.70	
69897	40.6	59.8	27.1	71.6	142.4	36.4		
	6.96	7.03	6.69	7.17	6.92	7.01	6.96	
76932	24.9	47.1	18.7	59.8	117.7	18.4		
	6.40	6.58	6.23	6.73	6.37	6.47	6.46	
142860	43.5	71.8	45.4	84.9	141.8	46.2		
	6.99	7.18	7.00	7.33	6.85	7.16	7.09	
165908	40.0	63.0	33.8	70.7	160.4	29.8		
	6.69	6.83	6.57	6.90	6.89	6.74	6.77	
182572	113.2	140.1	104.7	160.7	327.5	97.9		
	7.56	7.69	7.41	7.87	7.67	7.66	7.64	
201891	14.2	46.8	11.5	50.9	104.3	10.0: <sup>b</sup>		
	6.10	6.59	5.97	6.60	6.21	6.16:	6.27	
207978	23.9	46.3	22.0	49.7	115.9	22.4		
	6.72	6.92	6.68	6.93	6.62	6.78	6.78	
216385	49.8	73.6	43.1	83.1	159.6	45.9		
	7.10	7.22	6.99	7.30	7.04	7.17	7.14	
217107	116.1	128.1	104.5	142.8	345.9	100.5		
	7.64	7.56	7.44	7.69	7.75	7.72	7.63	
218470	45.4	65.5	36.1	75.7	153.5	42.7		
	7.25	7.33	7.09	7.44	7.19	7.25	7.26	
Sun	79.7	99.2	74.0	112.4	273.5	71.3		
	7.32	7.40	7.20	7.54	7.57	7.40	7.41	

TABLE 3 (continued)

HD	$W_\lambda$ (mÅ)						log Fe <sup>a</sup> (average)
	$\lambda$ (Å)	8582.271	8611.812	8621.618	8674.756	8688.642	
	log $gf$	-1.993	-1.900	-2.024	-1.850	-1.212	-0.360
$\chi$ (eV)	2.990	2.845	2.949	2.832	2.176	4.956	log Fe (average)
François (1988) sample:							
24616	...	...	...	90.7	...	37.7	6.25
				6.12		6.37	
59984	...	...	...	58.3	143.0	20.2	
				6.68	6.68	6.52	6.63
63077	...	...	...	57.3	143.0	20.0	
				6.60	6.56	6.46	6.54
69897	...	...	...	63.2	153.2	32.1	
				7.05	7.09	6.94	7.03
94028	...	...	...	21.9	85.0	...	
				6.10	6.00		6.05
104304	...	...	...	140.1	...	86.6	
				7.67		7.56	7.62
111721	...	...	...	61.9	131.0	15.0	
				6.08	6.00	5.94	6.01
132475	...	...	...	33.6	102.7	7.7	
				6.20	6.02	6.01	6.08
148816	...	...	...	50.5	...	19.2	
				6.56		6.48	6.52
157089	...	...	...	...	136.0	27.8	
					6.48	6.66	6.57
193901	...	...	...	...	140.4	15.6	
					6.45	6.31	6.38
201891	...	...	...	43.4	120.7	10.6	
				6.47	6.41	6.19	6.36
François (1987) sample:							
76932	...	...	...	53.0	113.0	16.0	
				6.62	6.27	6.40	6.51
88218	...	...	...	81.0	169.0	46.0	
				6.85	6.72	6.93	6.83
91324	...	...	...	62.0	...	32.0	
				6.92		6.89	6.91
102365	...	...	...	96.0	261.0	51.0	
				7.08	7.22	6.97	7.09
106516	...	...	...	50.0	116.0	21.0	
				6.90	6.70	6.72	6.77
114946	...	...	...	124.0	...	66.0	
				6.55		6.81	6.68
121384	...	...	...	95.0	...	43.0	
				6.52		6.61	6.57
136352	...	...	...	81.0	192.0	41.0	
				6.92	6.99	6.85	6.92
139211	...	...	...	74.0	168.0	49.0	
				7.25	7.22	7.25	7.24
188376	...	...	...	113.0	...	66.0	
				6.92		7.03	6.98
190248	...	...	...	125.0	...	79.0	
				7.50		7.43	7.47
203608	...	...	...	46.0	94.0	17.0	
				6.67	6.20	6.52	6.46
211998	...	...	...	54.0	127.0	9.0	
				6.04	5.74	5.82	5.87

<sup>a</sup> Equivalent widths and abundances are given in the first and the second of two entry rows for each star, respectively.<sup>b</sup> Since the line is broad,  $W_\lambda$  is measured by a direct integration.<sup>c</sup> Since the line is blended with other line(s),  $W_\lambda$  is measured by a direct integration.

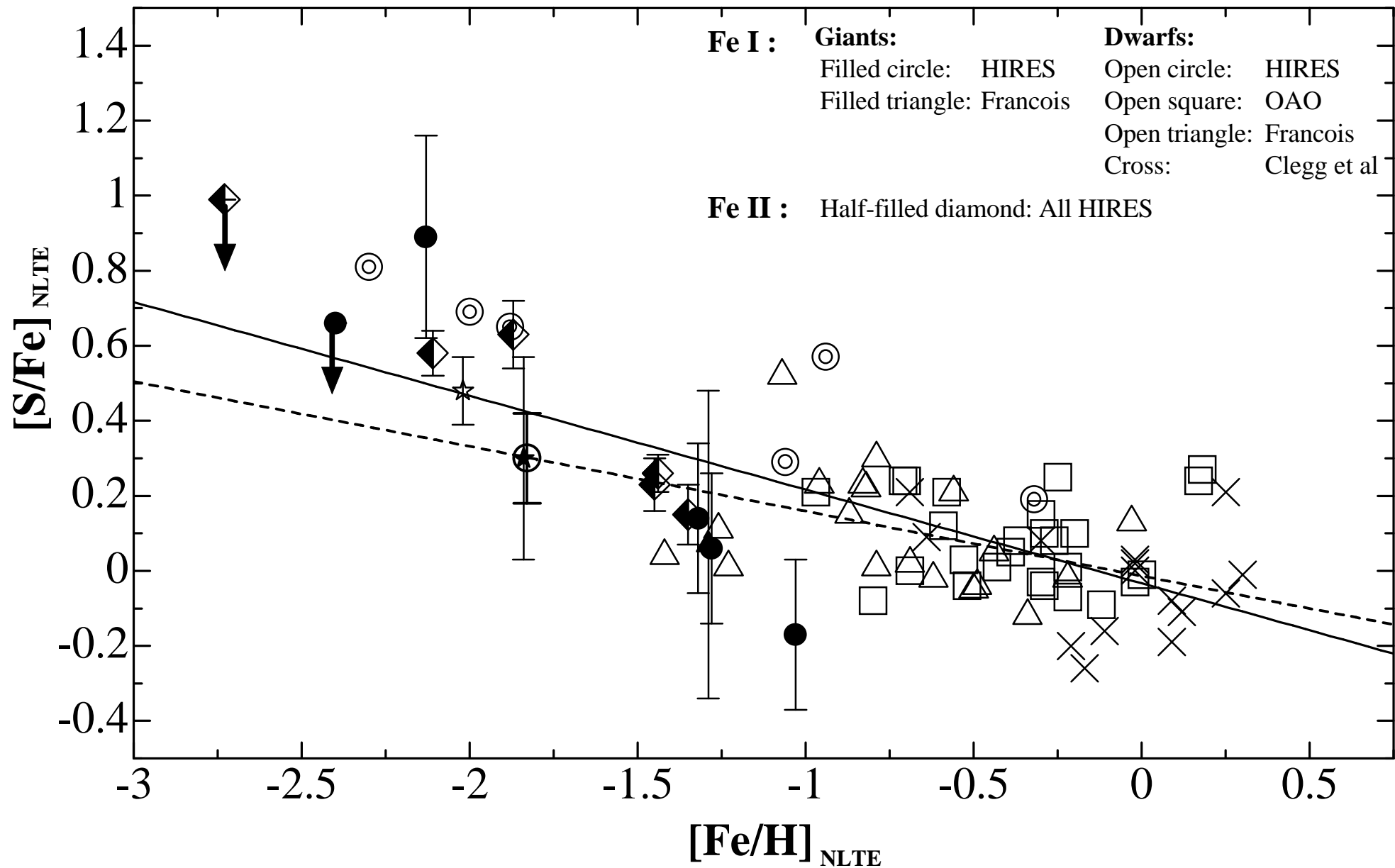


TABLE 4  
EQUIVALENT WIDTHS COMBINED WITH Si 8694 AND 8695 LINES  
AND LTE ABUNDANCES FOR THE OAO SAMPLE

HD	HR	$T_{\text{eff}}$	$\log g$	[Fe/H]	$\xi$ (km s $^{-1}$ )	$W_{\lambda}$ (mÅ)	$\log S$
3795	173	5330	3.80	-0.75	1.6	15.2	6.76
6582	321	5340	4.42	-0.85	0.8	10.0	6.76
13555	646	6470	3.90	-0.30	2.4	65.3	6.97
14412	683	5340	4.44	-0.55	0.8	12.6	6.88
15335	720	5840	3.89	-0.20	1.9	48.5	7.09
17948	860	6500	4.13	-0.30	2.1	54.5	6.92
18768	...	5750	3.84	-0.60	1.9	31.2	6.86
22484	1101	5960	4.02	-0.10	1.8	55.3	7.14
33256	1673	6440	3.99	-0.30	2.3	57.5	6.92
37495	1935	6350	3.74	-0.10	2.5	101.5	7.29
40136	2085	7190	4.15	-0.05	2.7	106.2	7.23
49933	2530	6590	4.15	-0.45	2.2	48.4	6.83
59984	2883	5890	3.92	-0.85	1.9	18.8	6.54
60532	2906	6150	3.69	-0.20	2.4	68.8	7.07
62301	...	5900	4.09	-0.70	1.7	26.4	6.76
69897	3262	6250	4.17	-0.25	1.9	48.5	6.95
76932	3578	5900	4.12	-0.80	1.7	11.3	6.35
142860	5933	6240	4.09	-0.15	2.0	60.3	7.03
165908	6775	5900	4.09	-0.60	1.7	25.2	6.73
182572	7373	5500	4.07	0.20	1.4	68.8	7.68
201891	...	5880	4.25	-1.00	1.5	13.0:	6.47:
207978	8354	6400	4.03	-0.55	2.2	36.7	6.69
216385	8697	6300	3.91	-0.25	2.3	65.6	7.04
217107	8734	5490	4.15	0.30	1.3	61.6	7.64
218470	8805	6600	4.01	-0.15	2.4	75.0	7.05
Sun	...	5780	4.44	0.00	1.2	42.6	7.22

: Uncertain value.

TABLE 5  
EQUIVALENT WIDTHS OF Si LINES AND LTE ABUNDANCES FOR THE SAMPLES OF HIRES,  
FRANÇOIS (1987, 1988), AND CLEGG ET AL. (1981)

HD	Si 8693.958		Si 8694.641		log S (average)
	$W_\lambda$ (mA)	log S	$W_\lambda$ (mA)	log S	
<b>HIRES sample:</b>					
44007	< 1.1	< 6.12	3.2	6.01	6.01
84937	< 1.4	< 5.89	3.4	5.70	5.70
88609	< 1.0	< 5.72	< 2.2	< 5.49	< 5.49
165195	< 0.7	< 6.08	2.0	5.98	5.98
175305	1.5:	6.08:	4.7	6.02	6.04
184266	4.1:	6.10:	13.9	6.12	6.11
<b>François (1988) sample:</b>					
24616	2.9	6.70	8.5	6.63	6.67
59984	4.4	6.55	13.4	6.49	6.52
63077	4.3	6.65	12.7	6.58	6.62
69897	...	...	26.2	6.75	6.75
94028	...	...	4.5	6.06	6.06
104304	16.5	7.68	27.1	7.41	7.55
111721	...	...	4.5	6.02	6.02
132475	...	...	4.2	6.00	6.00
148816	...	...	14.6	6.61	6.61
157089	5.7	6.77	16.2	6.69	6.73
193901	...	...	7.2	6.48	6.48
201891	...	...	7.1	6.29	6.29
<b>François (1987) sample:</b>					
76932	4.0	6.56	13.0	6.53	6.55
88218	8.0	6.91	21.0	6.83	6.87
91324	8.0	6.69	24.0	6.67	6.68
102365	4.0	6.78	12.0	6.73	6.76
106516	6.0	6.62	17.0	6.54	6.58
114946	3.0	6.64	7.0	6.46	6.55
121384	2.0	6.47	6.0	6.40	6.44
136352	...	...	12.0	6.69	6.69
139211	17.0	7.05	38.0	6.94	7.00
188376	6.0	6.88	16.0	6.80	6.84
190248	13.0	7.43	24.0	7.21	7.32
203608	4.0	6.51	13.0	6.49	6.50
211998	...	...	2.0	5.84	5.84
<b>Clegg et al. (1981) sample:</b>					
1461	18.0	7.49	36.0	7.35	7.42
4614	8.1	6.97	27.0	7.02	7.00
6582	...	...	7.0	6.69	6.69
10307	13.0	7.22	33.0	7.18	7.20
16895	22.0	7.27	51.0	7.22	7.25
30652	19.0	7.11	69.0	7.38	7.25
33256	12.0	6.80	37.0	6.83	6.82
34411	11.0	7.11	31.0	7.12	7.12
63077	5.0	6.72	13.0	6.59	6.67
82328	17.0	6.96	48.0	7.00	6.98
102870	22.0	7.28	48.0	7.20	7.24
114710	15.0	7.24	38.0	7.21	7.23
121370	...	...	80.0	7.59	7.59
128167	12.0	6.80	39.0	6.86	6.83
142860	14.0	6.98	48.0	7.12	7.05
145675	...	...	25.0	7.68	7.68
185144	...	...	7.0	6.78	6.78
207978	10.0	6.74	30.0	6.73	6.74
216385	18.0	7.03	43.0	6.96	7.00
224930	...	...	9.0	6.73	6.73

: Uncertain value and its weight is half for average.

TABLE 6  
RESULTS OF LTE AND NLTE ABUNDANCE ANALYSES OF THE HIRES SAMPLE AND THE GIANT STAR HD 111721

HD	[S/H] <sub>LTE</sub>	[Fe I/H] <sub>LTE</sub>	[Fe II/H] <sub>LTE</sub>	[S/Fe I] <sub>LTE</sub>	[S/Fe II] <sub>LTE</sub>	$\Delta(S)$	[Fe I/H] <sub>NLTE</sub>	[S/Fe I] <sub>NLTE</sub>	[S/Fe II] <sub>NLTE</sub>
Giants									
<b>HIRES sample:</b>									
44007	-1.20	-1.49	-1.45	0.29±0.20	0.25±0.07	-0.02	-1.28	0.06±0.20	0.23±0.07
88609	< -1.72	-2.69	-2.73	< 0.97	< 1.01	-0.02	-2.40	< 0.66	< 0.99
165195 <sup>a</sup>									
Ours	-1.23	-2.40	-1.87	1.17±0.27	0.64±0.09	-0.01	-2.13	0.89±0.27	0.63±0.09
Pap.I	-1.51	-2.09	-2.02	0.58±0.28	0.51±0.10	-0.03	-1.84	0.30±0.28	0.48±0.10
175305	-1.17	-1.21	-1.35	0.04±0.20	0.18±0.08	-0.03	-1.03	-0.17±0.20	0.15±0.08
184266	-1.10	-1.53	-1.44	0.43±0.20	0.34±0.05	-0.08	-1.32	0.14±0.20	0.26±0.05
<b>François (1988) sample:</b>									
111721	-1.19	-1.50	...	0.31±0.41	...	-0.03	-1.29	0.07±0.41	...
Dwarfs									
<b>HIRES sample:</b>									
84937	-1.51	-2.08	-2.11	0.57±0.12	0.60±0.06	-0.02	-1.83	0.30±0.12	0.58±0.06

<sup>a</sup> The atmospheric parameters  $T_{\text{eff}}/\log g/[\text{Fe}/\text{H}]$  of our and Paper I's models are 4190/1.00/-2.05 and 4450/1.10/-2.00, respectively.

TABLE 7  
RESULTS OF LTE AND NLTE ABUNDANCE ANALYSES OF THE DWARF SAMPLES OF OAO, FRANÇOIS, AND CLEGG ET AL.

HD	log S <sub>LTE</sub>	log Fe <sub>LTE</sub>	[S/H] <sub>LTE</sub>	[Fe I/H] <sub>LTE</sub>	[S/Fe I] <sub>LTE</sub>	Δ(S)	[S/Fe I] <sub>NLTE</sub>	[Fe I/H] <sub>NLTE</sub>
OAO sample:								
3795	6.76	6.56	-0.46	-0.85	0.39	-0.01	0.24	-0.71
6582	6.76	6.57	-0.46	-0.84	0.38	0.00	0.24	-0.70
13555	6.97	7.14	-0.25	-0.27	0.02	-0.04	-0.07	-0.22
14412	6.88	6.94	-0.34	-0.47	0.13	0.00	0.05	-0.39
15335	7.09	7.04	-0.13	-0.37	0.24	-0.02	0.15	-0.30
17948	6.92	7.05	-0.30	-0.36	0.06	-0.03	-0.04	-0.29
18768	6.86	6.71	-0.36	-0.70	0.34	-0.01	0.21	-0.58
22484	7.14	7.16	-0.08	-0.25	0.17	-0.02	0.10	-0.20
33256	6.92	7.04	-0.30	-0.37	0.07	-0.03	-0.03	-0.30
37495	7.29	7.10	0.07	-0.31	0.38	-0.07	0.25	-0.25
40136	7.23	7.39	0.01	-0.02	0.03	-0.06	-0.03	-0.02
49933	6.83	6.89	-0.39	-0.52	0.13	-0.03	0.01	-0.43
59984	6.54	6.58	-0.68	-0.83	0.15	-0.01	0.00	-0.69
60532	7.07	7.06	-0.15	-0.35	0.20	-0.04	0.10	-0.29
62301	6.76	6.70	-0.46	-0.71	0.25	-0.01	0.12	-0.59
69897	6.95	6.96	-0.27	-0.45	0.18	-0.02	0.08	-0.37
76932	6.35	6.46	-0.87	-0.95	0.08	-0.01	-0.08	-0.80
142860	7.07	7.09	-0.15	-0.32	0.17	-0.03	0.08	-0.26
165908	6.73	6.77	-0.49	-0.64	0.15	-0.01	0.03	-0.53
182572	7.68	7.64	0.46	0.23	0.23	-0.01	0.27	0.18
201891	6.47	6.27	-0.75	-1.14	0.39	-0.01	0.21	-0.97
207978	6.69	6.78	-0.53	-0.63	0.10	-0.03	-0.04	-0.52
216385	7.04	7.14	-0.18	-0.27	0.09	-0.03	0.01	-0.22
217107	7.64	7.63	0.42	0.22	0.20	-0.01	0.24	0.17
218470	7.05	7.26	-0.17	-0.15	-0.02	-0.04	-0.09	-0.12
Sun	7.22	7.41	0.00	0.00	0.00	-0.01	-0.01	0.00
François (1988) sample:								
24616	6.67	6.25	-0.54	-1.26	0.72	-0.01	0.52	-1.07
59984	6.52	6.63	-0.69	-0.88	0.19	-0.01	0.04	-0.74
63077	6.62	6.54	-0.59	-0.97	0.38	-0.01	0.22	-0.82
69897	6.75	7.03	-0.46	-0.48	0.02	-0.02	-0.09	-0.39
94028	6.06	6.05	-1.15	-1.46	0.31	0.00	0.11	-1.26
104304	7.55	7.62	0.34	0.11	0.23	-0.01	0.24	0.09
132475	6.00	6.08	-1.21	-1.43	0.22	-0.01	0.01	-1.23
148816	6.61	6.52	-0.60	-0.99	0.39	0.00	0.23	-0.83
157089	6.73	6.57	-0.48	-0.94	0.46	-0.01	0.30	-0.79
193901	6.48	6.38	-0.73	-1.13	0.40	0.00	0.23	-0.96
201891	6.29	6.36	-0.92	-1.15	0.23	-0.01	0.05	-0.98
François (1987) sample:								
76932	6.55	6.51	-0.66	-1.00	0.34	-0.01	0.17	-0.84
88218	6.87	6.83	-0.34	-0.68	0.34	-0.01	0.21	-0.56
91324	6.68	6.91	-0.53	-0.60	0.07	-0.02	-0.05	-0.50
102365	6.76	7.09	-0.45	-0.42	-0.03	-0.01	-0.12	-0.34
106516	6.58	6.77	-0.63	-0.74	0.11	-0.01	-0.02	-0.62
114946	6.55	6.68	-0.66	-0.83	0.17	-0.01	0.02	-0.69
121384	6.44	6.57	-0.77	-0.94	0.17	-0.01	0.01	-0.79
136352	6.69	6.92	-0.52	-0.59	0.07	-0.01	-0.04	-0.49
139211	7.00	7.24	-0.21	-0.27	0.06	-0.03	-0.02	-0.22
188376	6.84	6.98	-0.37	-0.53	0.16	-0.02	0.05	-0.44
190248	7.32	7.47	0.11	-0.04	0.15	-0.01	0.13	-0.03
203608	6.50	6.46	-0.71	-1.05	0.34	-0.01	0.15	-0.87
211998	5.84	5.87	-1.37	-1.64	0.27	-0.01	0.04	-1.42

TABLE 7 (continued)

HD	$\log S_{\text{LTE}}$	$\log \text{Fe I}_{\text{LTE}}$	$[\text{S}/\text{H}]_{\text{LTE}}$	$[\text{Fe I}/\text{H}]_{\text{LTE}}$	$[\text{S}/\text{Fe I}]_{\text{LTE}}$	$\Delta(\text{S})$	$[\text{S}/\text{Fe I}]_{\text{NLTE}}$	$[\text{Fe I}/\text{H}]_{\text{NLTE}}$
Clegg et al. (1981) sample:								
1461	7.42	...	0.21	0.32	-0.11	-0.02	-0.06	0.25
4614	7.00	...	-0.21	-0.37	0.16	-0.01	0.08	-0.30
6582	6.69	...	-0.52	-0.85	0.33	0.00	0.19	-0.71
10307	7.20	...	-0.01	-0.02	0.01	-0.01	0.00	-0.02
16895	7.25	...	0.04	-0.03	0.07	-0.03	0.03	-0.02
30652	7.25	...	0.04	0.11	-0.07	-0.03	-0.08	0.09
33256	6.82	...	-0.39	-0.26	-0.13	-0.03	-0.21	-0.21
34411	7.12	...	-0.09	0.12	-0.21	-0.01	-0.19	0.09
63077	6.67	...	-0.54	-0.77	0.23	-0.01	0.09	-0.64
82328	6.98	...	-0.23	-0.14	-0.09	-0.04	-0.16	-0.11
102870	7.24	...	0.03	0.15	-0.12	-0.02	-0.11	0.12
114710	7.23	...	0.02	-0.03	0.05	-0.02	0.02	-0.02
121370	7.59	...	0.38	0.39	-0.01	-0.09	-0.01	0.30
128167	6.83	...	-0.38	-0.26	-0.12	-0.03	-0.20	-0.21
142860	7.05	...	-0.16	-0.21	0.05	-0.02	-0.01	-0.17
145675	7.68	...	0.47	0.32	0.15	-0.01	0.21	0.25
185144	6.78	...	-0.43	-0.21	-0.22	0.00	-0.26	-0.17
207978	6.74	...	-0.47	-0.63	0.16	-0.02	0.03	-0.52
216385	7.00	...	-0.21	-0.24	0.03	-0.03	-0.05	-0.19
224930	6.73	...	-0.48	-0.83	0.35	0.00	0.21	-0.69

Notes — (1)  $[\text{S}/\text{H}]_{\text{LTE}}$  and  $[\text{Fe I}/\text{H}]_{\text{LTE}}$  of OAO sample are estimated relative to our  $\log S_{\text{LTE}}$  and  $\log \text{Fe I}_{\text{LTE}}$  of the Sun. (2) Log  $\text{Fe I}_{\text{LTE}}$  of Clegg et al. (1981) sample is not estimated due to no availability of observational line data, and  $[\text{Fe I}/\text{H}]_{\text{LTE}}$  is taken from Clegg et al. (1981). (3)  $[\text{Fe I}/\text{H}]_{\text{NLTE}}$  is estimated from our  $[\text{Fe I}/\text{H}]_{\text{LTE}}$  using the polynomial relation derived by Israeli et al. (2001).

TABLE 8  
ERROR ESTIMATION OF S AND Fe I ABUNDANCES FOR DWARFS SAMPLE

Abundance (dex)	$\Delta T_{\text{eff}}$ $\pm 100$ (K)	$\Delta \log g$ $\pm 0.15$ ( $\text{cm s}^{-2}$ )	$\Delta \xi$ $\pm 0.5$ ( $\text{km s}^{-1}$ )	Error <sup>a</sup> combined
[S/H]	$\mp 0.05$	$\pm 0.05$	$\mp 0.02$	$\pm 0.07$
[Fe I/H]	$\pm 0.08$	$\mp 0.01$	$\mp 0.10$	$\pm 0.13$
[S/Fe I]	$\mp 0.13$	$\pm 0.05$	$\mp 0.08$	$\pm 0.16$

<sup>a</sup> Estimated as a square root of quadratic sum of each error.